

From the Radiologic Pathology Archives¹

Intraventricular Neoplasms: Radiologic-Pathologic Correlation²

CME FEATURE

See www.rsna.org/education/Search/RG

LEARNING OBJECTIVES FOR TEST 2

After completing this journal-based SA-CME activity, participants will be able to:

- Discuss the differential diagnosis of intraventricular neoplasms.
- Describe the clinical and pathologic features of intraventricular neoplasms.
- List the imaging characteristics of intraventricular neoplasms.

TEACHING POINTS

See last page

Alice Boyd Smith, MD, Lt Col, USAF MC • James G. Smirniotopoulos, MD
Iren Horkanyne-Szakaly, MD

A variety of neoplasms may arise in the ventricular system. Intraventricular neoplasms may be discovered as an incidental finding at cross-sectional imaging or may manifest with varied symptoms depending on their location, including symptoms of increased intracranial pressure. These lesions may arise from various ventricular structures, including the ependymal lining (eg, ependymoma), subependymal layer (eg, subependymoma), or choroid plexus (eg, choroid plexus neoplasms), or they may have a cell of origin that has yet to be determined (eg, chordoid glioma). Other neoplasms involving the ventricular system include central neurocytoma, subependymal giant cell tumor, meningioma, rosette-forming glioneuronal tumor, and metastases. The differential diagnosis for intraventricular neoplasms can be broad, and many of them have similar patterns of signal intensity and contrast enhancement at imaging. However, the location of the lesion in the ventricular system—along with knowledge of the patient's age, gender, and underlying conditions—will help narrow the differential diagnosis.

Introduction

A variety of neoplasms may arise in the ventricular system. According to the lesion size and location, patients may be asymptomatic with the mass found as an incidental finding at cross-sectional imaging or may present with headaches, signs and symptoms of increased intracranial pressure, or a focal neurologic deficit. In addition, neoplasms involving the fourth ventricle may result in ataxia or paresis. Many of these lesions have similar patterns of signal intensity and contrast enhancement at imaging. However, the location of the lesion in the ventricular system—along with knowledge of the patient's age, gender, and underlying conditions—will help narrow the differential diagnosis.

Teaching Point

Abbreviations: CPC = choroid plexus carcinoma, CPP = choroid plexus papilloma, CSF = cerebrospinal fluid, H-E = hematoxylin-eosin, RGNT = rosette-forming glioneuronal tumor, SGCT = subependymal giant cell tumor, TS = tuberous sclerosis, WHO = World Health Organization

RadioGraphics 2013; 33:21–43 • Published online 10.1148/radiographics.rs31125192 • Content Codes: CT MR NR OI

¹Supported by the American Institute for Radiologic Pathology (AIRP), the Joint Pathology Center (JPC), and Uniformed Services University of the Health Sciences (USU).

²From the Department of Radiology and Radiological Sciences, Uniformed Services University of the Health Sciences, 4301 Jones Bridge Rd, Bethesda, MD 20814-4799 (A.B.S., J.G.S.); American Institute for Radiologic Pathology, Silver Spring, Md (A.B.S.); and Joint Pathology Center, Silver Spring, Md (I.H.S.). Received September 5, 2012; revision requested October 8 and received October 24; accepted November 4. For this journal-based SA-CME activity, the authors, editor, and reviewers have no relevant relationships to disclose. Address correspondence to A.B.S. (e-mail: absmith@pobox.com).

The opinions or assertions contained herein are the private views of the authors and are not to be construed as official or as reflecting the views of the Departments of the Air Force, Army, or Defense.

In this article, we describe the clinical and imaging features of intraventricular neoplasms with emphasis on pathologic correlation. Specific topics discussed include ventricular anatomy, ependymoma, subependymoma, central neurocytoma, subependymal giant cell tumor (SGCT), choroid plexus neoplasms, meningioma, chordoid glioma, rosette-forming glioneuronal tumor (RGNT), and metastases and other intraventricular neoplasms.

Ventricular Anatomy

The differential diagnosis of intraventricular neoplasms is broad. To understand the different entities that can occur in an intraventricular location, it is important to understand the embryology, anatomy, and histologic structure of the ventricular system.

The cerebral ventricles begin as ependymal-lined outpouchings from the cranial end of the neural tube, which are called the telencephalic vesicles. The choroid plexus develops from an invagination of primitive pia-arachnoid and vessels into these vesicles, thus creating the choroidal fissures. The epithelial lining of the ventricles is composed of ependymal cells, which are the cell of origin of the ependymoma. Subjacent to the ependymal lining is a layer of subependymal plate composed of glial cells, from which subependymomas are thought to arise.

The septum pellucidum is also lined by glial cells and residual neuronal precursor cells, from which the central neurocytoma may arise. The very vascular choroid plexus produces cerebrospinal fluid (CSF) and may give rise to primary neoplasms of the choroid plexus (choroid plexus papilloma, atypical choroid plexus papilloma, choroid plexus carcinoma); owing to its vascular supply, it may contribute to deposition of metastases in this location. Arachnoidal cap cells, which make up the arachnoid granulations, may become trapped within the choroid plexus during embryologic development; these cells can give rise to meningiomas.

Ependymoma

Ependymomas account for 3%–5% of intracranial neoplasms (1). They are generally well-circumscribed glial tumors with ependymal differentiation that arise from the ependymal cells of the ventricular wall. These lesions can occur either supratentorially (40% of cases) or within the posterior fossa (60%) (2). More than one-half of supratentorial ependymomas are intraparen-

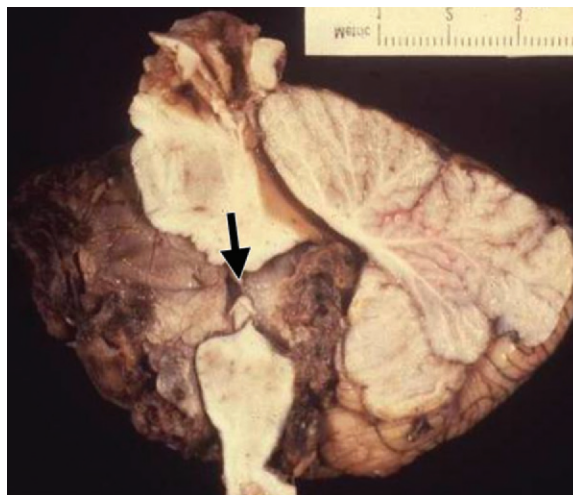


Figure 1. Ependymoma of the fourth ventricle in a 2-year-old girl. Photograph of a midline sagittal plane section through the posterior fossa shows a mass that extends from the fourth ventricle through the foramen of Luschka (arrow) into the cerebellopontine angle. (Scale is in centimeters.)

chymal, with the remainder being intraventricular (3,4). One theory for the origin of the intraparenchymal lesions is that they arise from embryonic rests of ependymal tissue trapped in the developing cerebral hemispheres (5). Rare reports exist of extraaxial intracranial ependymomas (6).

Ependymomas can occur in any age group but are more common in younger patients. Those that occur in the posterior fossa are more common in children (mean age, 6 years), whereas the mean age for supratentorial lesions is 18–24 years (1). Ependymomas are the third most common brain neoplasm in children, behind medulloblastoma (primitive neuroectodermal tumor) and astrocytic tumors (7). Presenting symptoms depend on the location: Those that occur in the fourth ventricle typically manifest with symptoms of increased intracranial pressure due to obstruction, ataxia, or paresis, whereas supratentorial lesions manifest as headache, focal neurologic deficit, or seizure (5).

The 5-year survival rate in children is reported to be 50%–75% (8). Children have a less favorable prognosis than older patients, in part due to the higher prevalence of fourth ventricle lesions; in addition, there is a greater predilection for the anaplastic form in the pediatric population (5). Surgery plays an important role in treatment, but surgical resection is often difficult due to adherence and the infiltrating nature of the tumor. If the resection is subtotal, the ependymoma tends to recur. With recurrence the prognosis is very poor, with a mortality rate of approximately 90% (8).

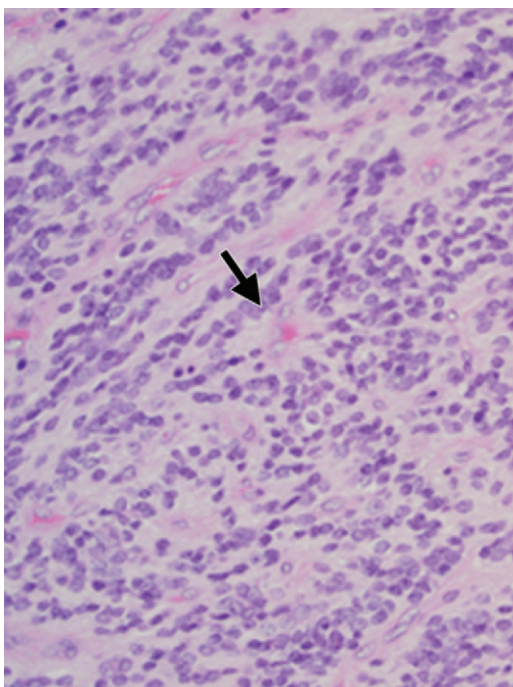


Figure 2. Grade II ependymoma in a 2-year-old girl. Photomicrograph (original magnification, $\times 100$; hematoxylin-eosin [H-E] stain) shows a moderately cellular glial neoplasm with a perivascular pseudorosette (arrow). No mitotic activity is present.

Pathologic Findings

Ependymomas are classified as either World Health Organization (WHO) grade II (low-grade, well-differentiated) or grade III (anaplastic) neoplasms. At gross inspection, these are soft “plastic” neoplasms. In the region of the fourth ventricle, they may extend through the foramen of Luschka into the cerebellopontine angle cistern or through the foramen magnum (Fig 1).

WHO grade II ependymomas are moderately cellular tumors, with rare mitotic figures. The classic histologic findings in ependymomas are perivascular pseudorosettes and true ependymal rosettes (Fig 2). WHO grade III ependymomas demonstrate increased cellularity with brisk mitotic activity, along with ependymal differentiation. Frequently, microvascular proliferation and necrosis are seen.

Imaging Features

Ependymomas frequently demonstrate cystic components and areas of small chunky calcification. Occasionally, intratumoral hemorrhage may be seen. At computed tomography (CT), the soft-tissue portion is commonly hypo- to isoattenuating (Fig 3).

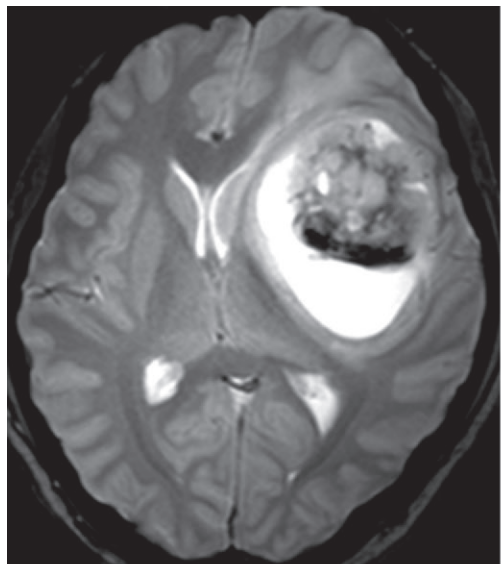


Figure 3. Ependymoma in a 2-year-old girl with ataxia and headaches. Nonenhanced CT image shows a solid and cystic lesion that arises from the fourth ventricle and extends through the foramen of Luschka into the cerebellopontine angle. The solid portion is slightly hyperattenuating relative to the adjacent cerebellum. Areas of calcification are also present. The mass results in hydrocephalus, with dilatation of the third and lateral ventricles.

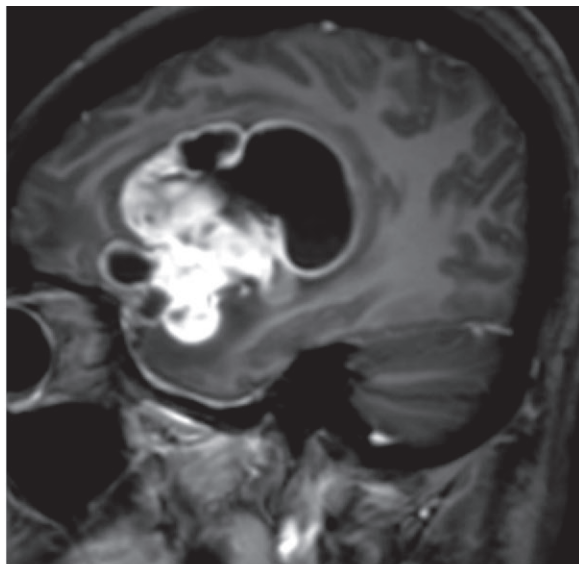
At magnetic resonance (MR) imaging, they are iso- to hypointense on T1-weighted images and iso- to hyperintense on T2-weighted images. Heterogeneous enhancement is seen on contrast material-enhanced images. Blooming may be seen on T2*-weighted images if calcification or hemorrhage is present. Findings on diffusion-weighted images are variable. Reduced diffusion may be seen in the soft-tissue component of some ependymomas, a finding that most likely reflects higher cellularity in some neoplasms (4).

Intraparenchymal lesions are typically large at presentation, with up to 94% being over 4 cm in size at the time of diagnosis (9). Many intraparenchymal supratentorial ependymomas have a large cystic component. They may also have a “cyst and mural nodule” appearance, for which the differential diagnosis includes pilocytic astrocytoma, pleomorphic xanthoastrocytoma, and ganglioglioma; however, they may be completely solid as well (9) (Fig 4). The cystic component tends to be similar in signal intensity on T1- and T2-weighted images, but it may not be completely suppressed on T2-weighted fluid-attenuated inversion-recovery (FLAIR) images due to proteinaceous content.

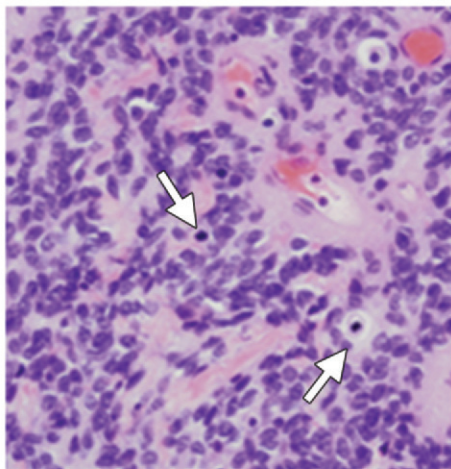
Figures 4, 5. (4) Intraparenchymal anaplastic ependymoma in a 24-year-old woman with a 1-month history of headaches. (a) Axial T2-weighted image shows a cystic neoplasm with a solid, heterogeneous nodule along its anterior border. A linear rim of low signal intensity secondary to calcification is noted along the posterior aspect of the nodule. The solid portion is isointense to gray matter. (b) Sagittal contrast-enhanced T1-weighted image shows enhancement of the nodular component and the cyst walls. (c) Photomicrograph (original magnification, $\times 100$; H-E stain) shows a highly cellular neoplasm composed of glial cells with multiple mitotic figures (arrows). (5) Lateral ventricle ependymoma in a 15-year-old girl. Axial CT image shows a solid mass with focal areas of calcification in the left lateral ventricle. Vasogenic edema is present in the left frontal lobe, and hydrocephalus is also seen.



4a.



4b.



4c.

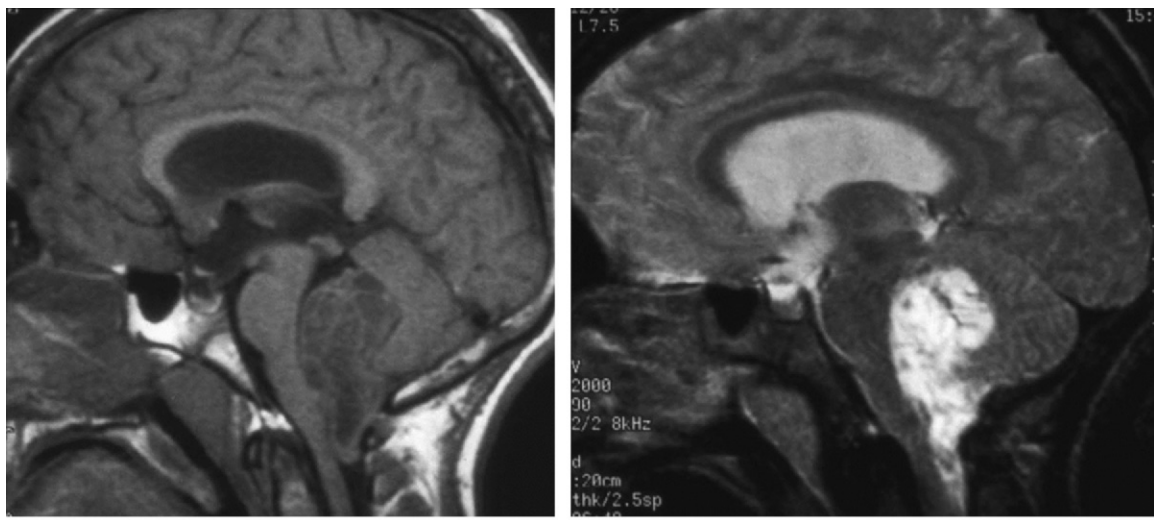


5.

Intraventricular lesions may extend into adjacent brain, and there may be vasogenic edema in the adjacent periventricular white matter (Fig 5). Ependymomas involving the fourth ventricle tend to fill the ventricle—like a plaster cast—and may extend through the foramen of Luschka, foramen of Magendie, or foramen magnum. This finding is highly suggestive of an ependymoma (5) (Fig 6) but is not pathognomonic, since occasionally medulloblastomas may extend through the foramen magnum.

Intraventricular ependymomas are associated with a small risk of spread throughout the CSF. Evidence of CSF spread at cytologic analysis was reported in 12% of cases in one series of 754 patients (10). Therefore, imaging of the entire neuroaxis should be performed to assess for CSF dissemination.

Figure 6. Fourth ventricle ependymoma in a 6-year-old boy. (a) Sagittal T1-weighted image shows a hypointense lesion filling and conforming to the fourth ventricle with extension through the foramen magnum. (b) On a T2-weighted image, the neoplasm is hyperintense. Resultant hydrocephalus is present.



a.

b.

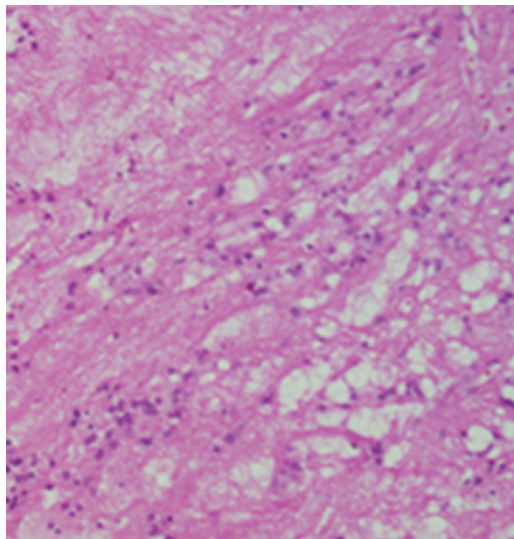


Figure 7. Lateral ventricle subependymoma in a 36-year-old man. Photomicrograph (original magnification, $\times 40$; H-E stain) shows a microcystic lesion with a dense fibrillary matrix and no evidence of significant vascularity. No mitoses are present.

Subependymomas have a male predominance (male-to-female ratio, 2.3:1), and 82% occur in patients older than 15 years (1). Most patients (60%) are asymptomatic; in those who are symptomatic, the symptoms are most commonly related to hydrocephalus (11). The classic scenario is a middle-aged man with an incidental finding of an intraventricular neoplasm at imaging. The prognosis for these patients is good, and recurrence after surgical resection is rare (1).

Subependymoma

Subependymomas account for 0.2%–0.7% of intracranial neoplasms; however, this may be an underestimate, since often they are asymptomatic and found incidentally (11). It is thought that they arise from the subependymal glial layer surrounding the cerebral ventricles, but the exact histogenesis remains uncertain (12). Most of these lesions occur in the fourth ventricle (50%–60%) and lateral ventricles (30%–40%) (13,14). Rarely, they may arise from other intraventricular sites or within the central canal of the spinal cord (11). The majority are less than 2 cm in size, but symptomatic lesions tend to be 4 cm or greater in size (11).

Pathologic Findings

Subependymomas are WHO grade I neoplasms with ependymal differentiation. These well-circumscribed lesions are typically attached to the ventricle wall by a narrow pedicle. Histologic analysis reveals a finely fibrillary background and occasional clustering of small, uniform, cytologically bland ependymoma-like nuclei. They often demonstrate numerous small cysts, especially in those lesions that originate from the lateral ventricle (Fig 7). These lesions do not have any significant vascularity, and mitotic activity is low or absent (12).

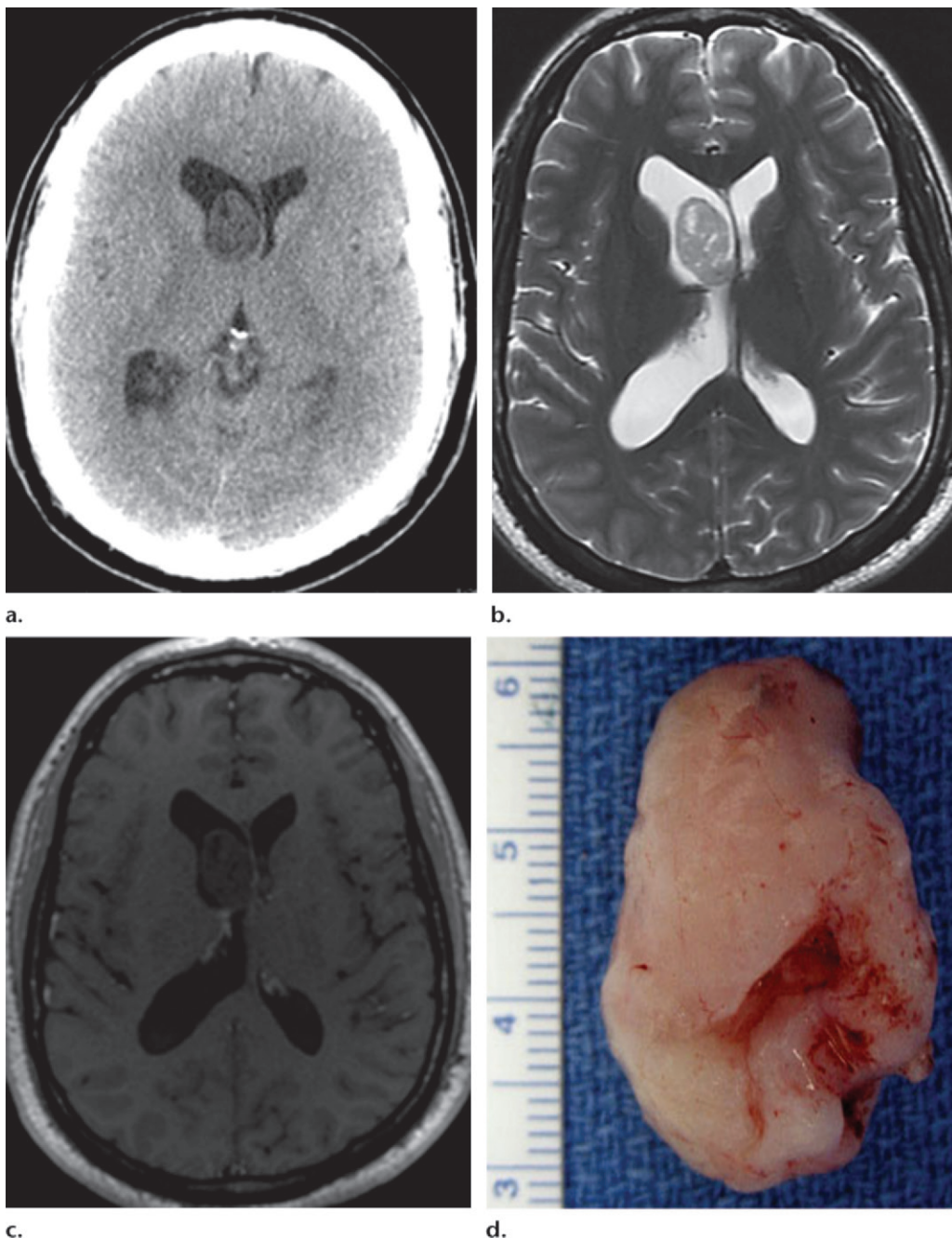


Figure 8. Lateral ventricle subependymoma in a 44-year-old man with a history of headaches. **(a)** Axial nonenhanced CT image shows a well-circumscribed hypoattenuating lesion arising in the anterior horn of the right lateral ventricle near the foramen of Monro. Small cysts are present. No peritumoral edema is noted in the adjacent brain. **(b)** Axial T2-weighted image shows a hyperintense mass without evidence of peritumoral edema. **(c)** Contrast-enhanced T1-weighted image shows no associated enhancement. Mild hydrocephalus is present. **(d)** Photograph of the resected specimen shows a well-circumscribed 3-cm lesion. (Scale is in centimeters.)

Occasionally, these neoplasms demonstrate aspects of a cellular ependymoma. Such cases are classified as mixed ependymoma-subependymoma, are graded on the basis of the ependymoma component, and tend to have an ependymoma-like clinical course (12).

Imaging Features

Subependymomas are well-circumscribed lesions that are hypo- to isoattenuating at CT (Fig 8a). Cystic degeneration is common, and calcification may be seen in the lesion. Intratumoral hemorrhage may also occur. MR imaging reveals a lesion that is hypo- to isointense relative to white matter and hyperintense on T2-weighted images

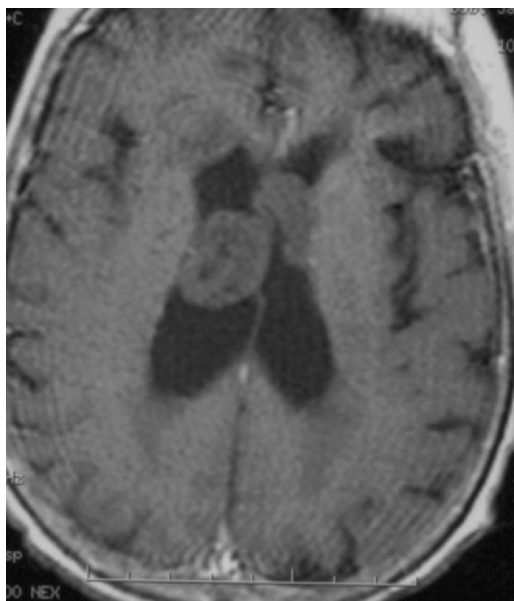


Figure 9. Subependymomas in a 73-year-old woman with behavioral changes and emesis.

Contrast-enhanced T1-weighted image shows two nonenhancing lesions in the right lateral ventricle and one in the left. The lesions appear to be attached to the ventricle wall, and small cysts are present. Lack of enhancement allows differentiation of subependymomas from more vascular multifocal lesions such as metastases.

(Fig 8b). Enhancement is variable, with most lesions demonstrating no or minimal enhancement; less commonly, there is moderate but typically heterogeneous enhancement (1,15) (Fig 8c).

Unlike with ependymomas, no invasion into the brain parenchyma occurs, and it is rare for there to be adjacent T2 hyperintensity in the periventricular white matter (11). No CSF dissemination occurs. Rarely, multiple subependymomas may be present (Fig 9), but the lack of significant enhancement helps differentiate these lesions from other multifocal processes such as metastases. Angiography reveals an avascular or hypovascular mass, a finding that reflects the relatively avascular nature of these lesions at histologic analysis (15).

Central Neurocytoma

Central neurocytomas account for 0.25%–0.5% of intracranial tumors and were described in 1982 (16). The origin of these tumors is unclear, but results of cell-culture investigations suggest they arise from bipotential progenitor cells that are capable of both neuronal and glial differentiation (17). Central neurocytomas occur in the lateral ventricle with or without extension into the third ventricle and arise from the septum pellucidum or ventricular wall (18) (Fig 10). Extraventricular neurocytomas are also described and arise in the brain parenchyma, cerebellum, and spinal cord.

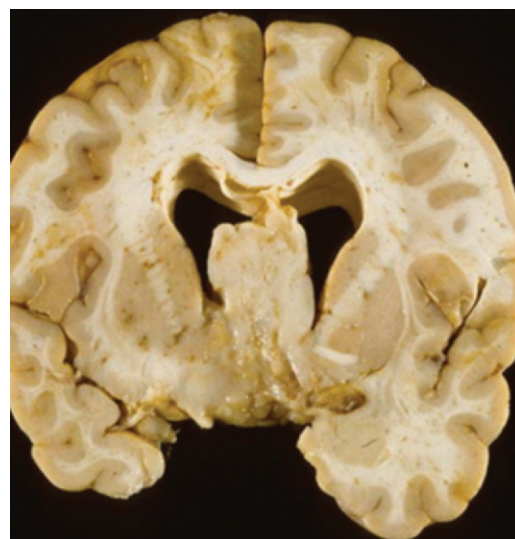


Figure 10. Central neurocytoma. Autopsy photograph of a brain shows a mass attached to the septum pellucidum.

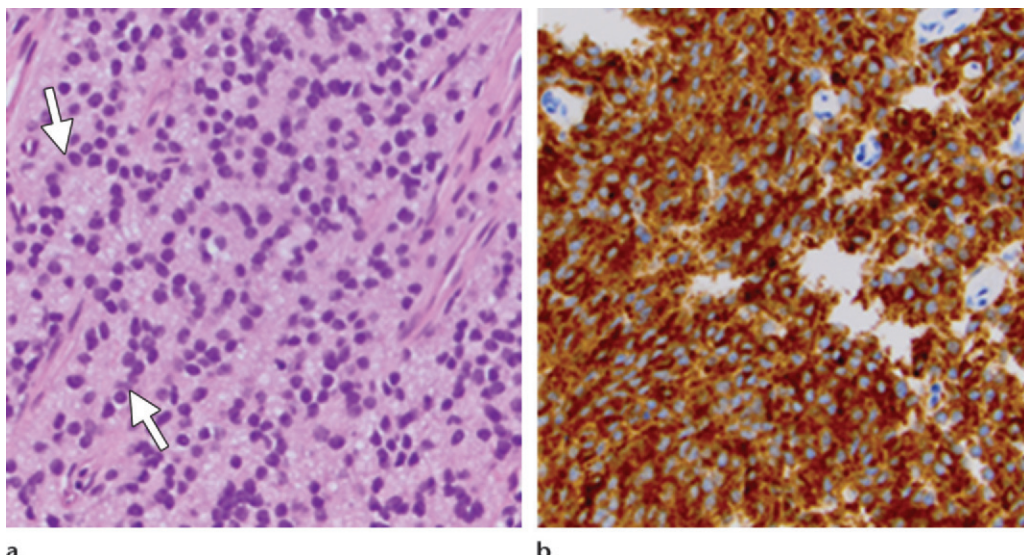
The term *central neurocytoma* is reserved for neurocytomas that occur in the ventricular system.

The mean patient age is 29 years, but a wide age range is reported, from 8 days to 67 years; there is no gender predilection (17). Patients typically present with symptoms of increased intracranial pressure. Gross total resection is usually curative, but recurrence and CSF dissemination have been reported (19,20).

Pathologic Findings

Central neurocytomas are WHO grade II lesions. They were originally classified as WHO grade I, but in 1993 they were upgraded to grade II due to reports of more aggressive behavior in some cases (21). At gross analysis, central neurocytomas are gray friable lesions often containing calcification or hemorrhage. These neoplasms typically have a benign histologic appearance, featuring solid sheets or large lobules of small round to ovoid neoplastic cells with a delicate vascular network and intervening irregular patches of fibrillary neuropil. Atypical forms demonstrate increased mitoses, atypia, and in some cases microvascular proliferation and necrosis.

Various architectural patterns may be observed, including an oligodendrogloma-like appearance and neurocytic rosettes. In fact, these tumors were mistakenly classified as “intraventricular oligodendrogloma” before the 1980s. The presence of pineocytomatous rosettes allows differentiation of central neurocytoma from oligodendrogloma (1) (Fig 11a). Central neurocytomas usually express immunoreactivity for synaptophysin and



a.

b.

Figure 11. Central neurocytoma. **(a)** Photomicrograph (original magnification, $\times 100$; H-E stain) shows sheets of neoplastic cells with round, regular nuclei in a fibrillary matrix. Pineocytomatous rosettes are noted (arrows). **(b)** Photomicrograph (original magnification, $\times 100$) after immunostaining for synaptophysin shows marked positivity (areas of brown staining).

neuron-specific enolase, which are both markers of neuronal differentiation, and strong staining for synaptophysin is reported to be the most reliable diagnostic marker (Fig 11b) (18,22).

Imaging Features

Central neurocytomas are well-circumscribed, lobulated masses that frequently have cystlike areas. Up to 50% may contain calcification, and hemorrhage may rarely be seen (17). At CT, these lesions are hyperattenuating (Fig 12a). At MR imaging, central neurocytomas are isointense to gray matter on T1-weighted images and hyperintense on T2-weighted images (Fig 12b). These lesions may have a “bubbly” appearance due to the presence of multiple cysts. At contrast-enhanced imaging, the enhancement pattern is variable, but moderate to strong enhancement is typically seen (18) (Fig 12c). Prominent flow voids may be noted, and increased T2 signal intensity may be seen in the adjacent periventricular white matter.

Recent evaluation with MR spectroscopy has revealed the presence of glycine (3.55 ppm) within central neurocytomas, a finding that may help differentiate them from other intraventricular neoplasms (23–25).

Subependymal Giant Cell Tumor

SGCT is the most common cerebral neoplasm in patients with tuberous sclerosis (TS), developing in up to 16% of cases (26). It has previously been referred to as *subependymal giant cell astrocytoma*,

but recent pathologic studies have revealed that it is a glioneuronal tumor; thus, the trend is away from use of the term *subependymal giant cell astrocytoma* (27,28). TS is a neurocutaneous disorder occurring in one in 6000 births that results from inactivating mutations in one of two tumor suppressor genes: *TSC1* (chromosome 9) or *TSC2* (chromosome 16) (29). SGCT is considered pathognomonic for TS, but there have been rare reports of SGCT in patients without manifestations of TS (30). However, these cases likely represent somatic mosaicism of the *TSC* gene (31).

There is a wide age range for presentation, from birth to the 5th decade (mean age, 11 years) (1,26). These lesions arise near the foramen of Monro (Fig 13a), and it has been proposed that SGCTs arise from a subependymal nodule (32). Uncommonly, SGCTs have been reported to arise in other locations, including extraventricularly (33). They are slow-growing lesions, and due to their location they commonly manifest with symptoms of increased intracranial pressure from obstructive hydrocephalus.

Indications for resection include increasing tumor size, hydrocephalus, a new focal neurologic deficit, or symptoms of increased intracranial pressure. Surgery is usually curative, but rarely seeding of the CSF pathways and recurrence after resection have been reported (34,35). Surveillance imaging studies are recommended every 2 years for patients with the *TSC2* mutation and every 3 years for patients with the *TSC1* mutation (36). Once an SGCT is identified, follow-up imaging at yearly intervals is recommended (37).

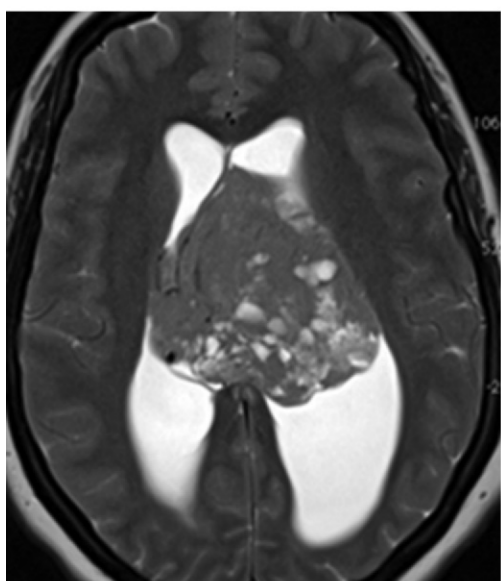
Teaching Point

Teaching Point

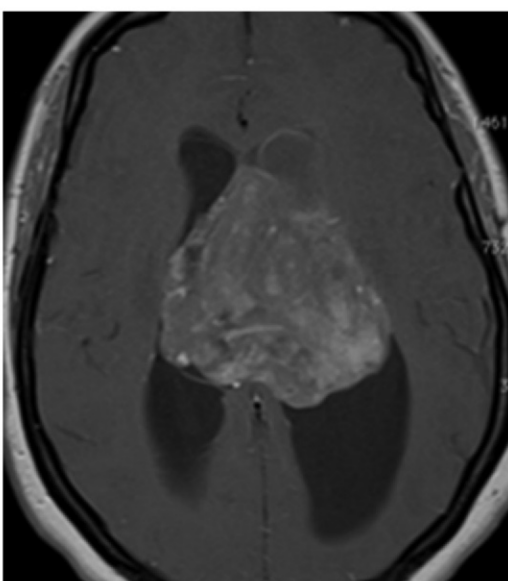


a.

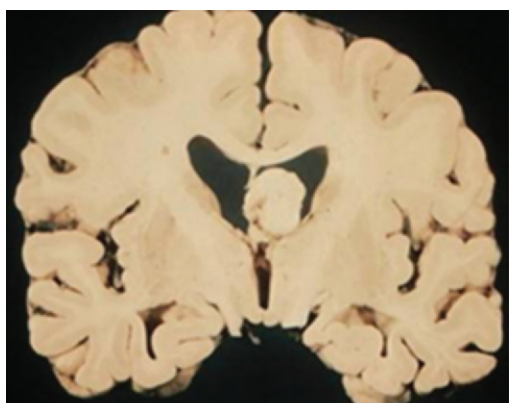
Figure 12. Central neurocytoma in a 27-year-old woman with a 4-month history of headaches. **(a)** Axial nonenhanced CT image shows a lesion located centrally within the lateral ventricles. Small foci of hyperattenuation consistent with calcification are present, as well as foci of hypoattenuation consistent with cystic areas. Hydrocephalus is present. **(b)** Axial T2-weighted image shows a large mass that is slightly hyperintense to gray matter located centrally around the septum pellucidum. Foci of hyperintensity consistent with cystic regions are noted. No increased signal intensity is appreciated in the adjacent brain parenchyma. **(c)** Axial contrast-enhanced T1-weighted image shows moderate heterogeneous enhancement.



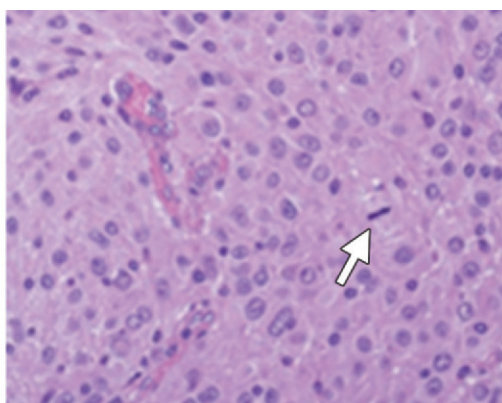
b.



c.



a.



b.

Figure 13. SGCT. **(a)** Autopsy photograph of a brain shows a mass located adjacent to the foramen of Monro. **(b)** Photomicrograph (original magnification, $\times 100$; H-E stain) shows large cells with abundant cytoplasm. A mitotic figure is present (arrow).

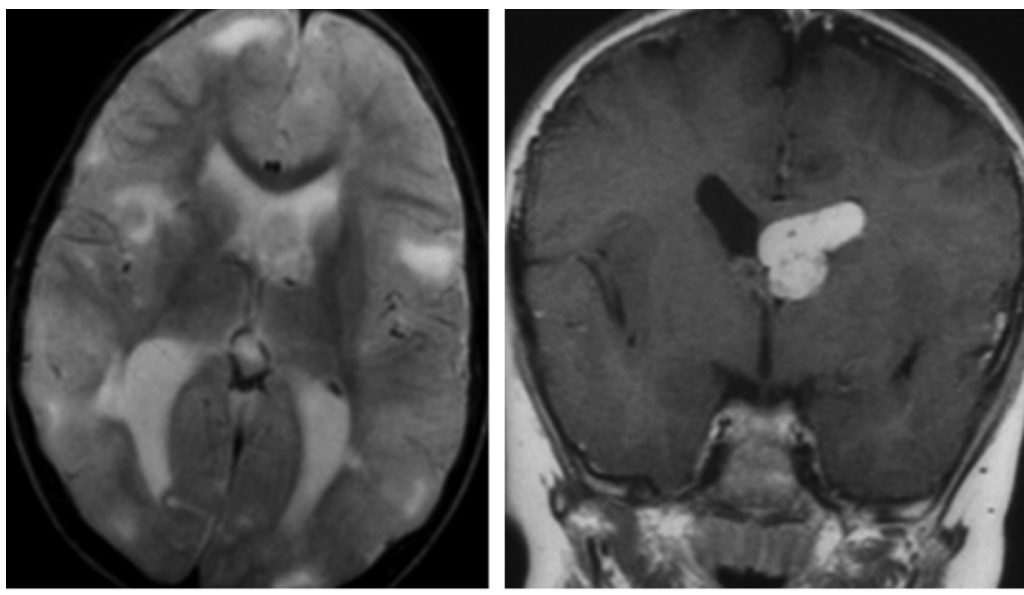


Figure 14. SGCT in a 9-year-old boy with TS. **(a)** Axial T2-weighted image shows a hyperintense mass near the foramen of Monro. Multiple subcortical focal areas of T2 hyperintensity are noted, which are consistent with subcortical tubers. **(b)** Coronal contrast-enhanced T1-weighted image shows avid enhancement of the neoplasm.

Pathologic Findings

SGCT is a WHO grade I lesion that macroscopically appears as well-circumscribed solid intraventricular neoplasms occurring near the foramen of Monro. Histologic evaluation reveals large cells resembling astrocytes or ganglion cells with abundant cytoplasm. The cells may be polygonal, epithelioid, or spindle shaped (Fig 13b) (38). Nuclear pleomorphism, increased mitotic activity, occasional endothelial proliferation, and necrosis may occur but are not indicative of malignant transformation and have no implication for prognosis (34).

The histogenesis of SGCT is unclear, but there is evidence to support both neuronal and astrocytic lineage. Immunohistochemical staining reveals markers for both glial and neuronal proteins (34).

Imaging Features

Imaging reveals a well-circumscribed lesion that is typically larger than 1 cm and most commonly located near the foramen of Monro. Other subependymal nodules may be noted. Owing to its location, hydrocephalus may be seen. Variable degrees of calcification may be present, and hemorrhage may occasionally be seen. At CT, SGCTs are hypo- to isoattenuating. MR imaging reveals a lesion that is hypo- to isointense to gray matter on T1-weighted images and iso- to hyperintense on T2-weighted images. At contrast-enhanced imaging, the lesions avidly enhance (Fig 14).

Choroid Plexus Neoplasms

Choroid plexus tumors account for 2%–4% of pediatric brain tumors, 0.5% of adult brain tumors, and up to 20% of pediatric neoplasms occurring in the 1st year of life (39,40). These neoplasms arise anywhere that choroid plexus is located and develop from the choroid plexus epithelium. They most commonly occur in the atrium of the lateral ventricle (50% of cases). Forty percent occur in the fourth ventricle, 10% in the third ventricle, and approximately 5% in more than one location (41).

Fourth ventricle lesions are more common in males (male-to-female ratio, 3:2), but there is no gender predilection for lateral ventricle lesions (40). Lateral ventricle lesions are more common in children (80% of cases), whereas fourth ventricle lesions are evenly distributed among all age groups (40). Rare cases of extraventricular choroid plexus tumors have been reported (42,43). Association of these neoplasms with several syndromes, including Aicardi and Li-Fraumeni syndromes, has been demonstrated (40,44,45).

Choroid plexus neoplasms may be subdivided on the basis of histologic findings into choroid plexus papilloma (CPP) (WHO grade I), atypical CPP (WHO grade II), or choroid plexus carcinoma (CPC) (WHO grade III). CPPs outnumber CPCs by a ratio of 5:1 (40). Transformation from a CPP to a CPC has been reported in a small number of cases (46).

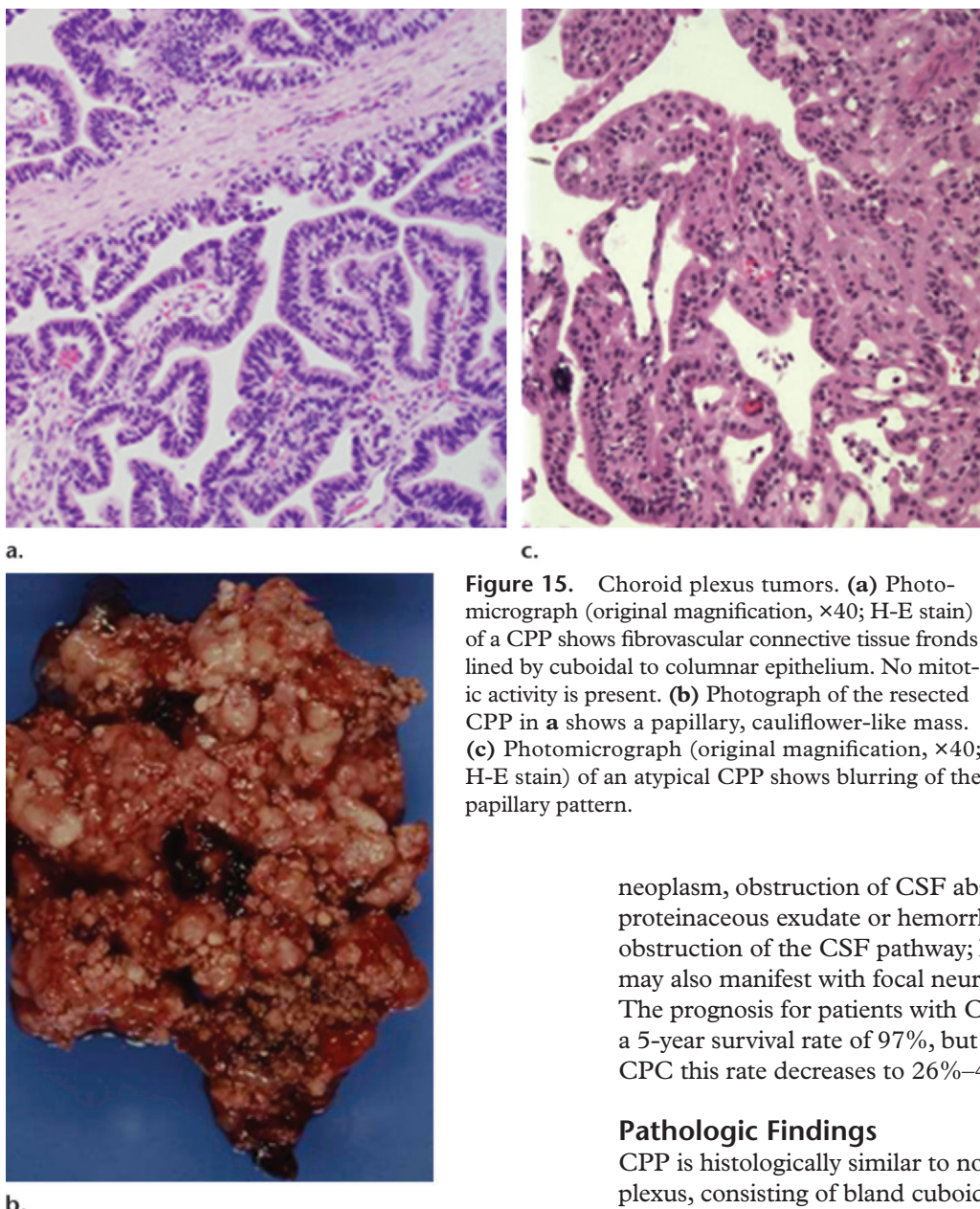


Figure 15. Choroid plexus tumors. **(a)** Photomicrograph (original magnification, $\times 40$; H-E stain) of a CPP shows fibrovascular connective tissue fronds lined by cuboidal to columnar epithelium. No mitotic activity is present. **(b)** Photograph of the resected CPP in **a** shows a papillary, cauliflower-like mass. **(c)** Photomicrograph (original magnification, $\times 40$; H-E stain) of an atypical CPP shows blurring of the papillary pattern.

neoplasm, obstruction of CSF absorption due to proteinaceous exudate or hemorrhage, or direct obstruction of the CSF pathway; however, CPCs may also manifest with focal neurologic deficits. The prognosis for patients with CPP is good, with a 5-year survival rate of 97%, but for those with CPC this rate decreases to 26%–43% (40,51).

Pathologic Findings

CPP is histologically similar to normal choroid plexus, consisting of bland cuboidal to columnar epithelial cells surrounding a delicate fibrovascular stalk (Fig 15a). At gross inspection, these are discrete, well-circumscribed, often papillary masses (Fig 15b). Mitotic activity is low; brain invasion and necrosis may occur but are uncommon (40). Hemorrhage and cyst formation may be seen in all of the choroid plexus neoplasms.

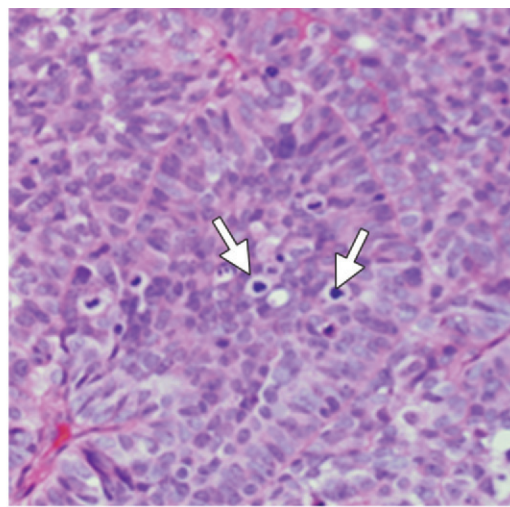
Atypical CPPs demonstrate two or more mitoses per 10 randomly selected high-power fields. Up to two of the following features may be present but are not required for diagnosis: increased cellularity, nuclear pleomorphism, blurring of the papillary pattern (Fig 15c), and areas of necrosis (40).

CPC is a rare tumor that shows frank signs of malignancy. Diagnosis of CPC requires the presence of at least four of the following features:

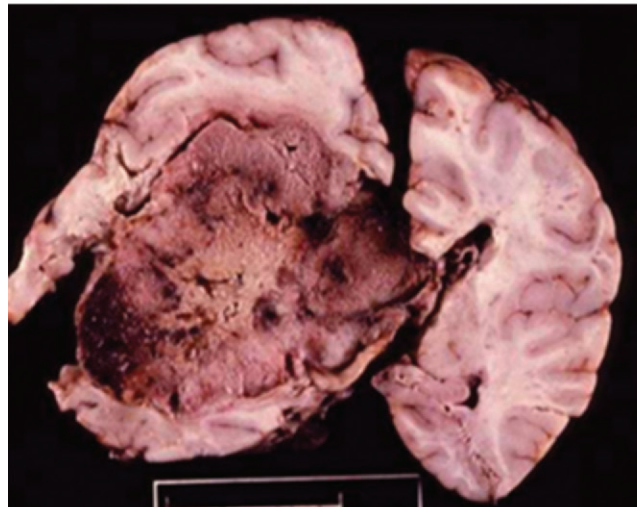
CPP and atypical CPP have a broad age distribution, although they are more common in the pediatric population; conversely, CPC is found almost entirely in the pediatric population (median age, 26–32 months) (40). Rare cases of CPC in adults have been reported; however, whenever this potential diagnosis is raised in an adult patient, it is imperative that metastatic carcinoma to the choroid plexus be ruled out, as these two entities may appear similar at histologic analysis and metastasis is far more common (47–49).

Chromosomal rearrangements and imbalances differ between CPP and CPC, suggesting different genetic pathways in development (50). Patients frequently present with hydrocephalus, which results from either overproduction of CSF by the

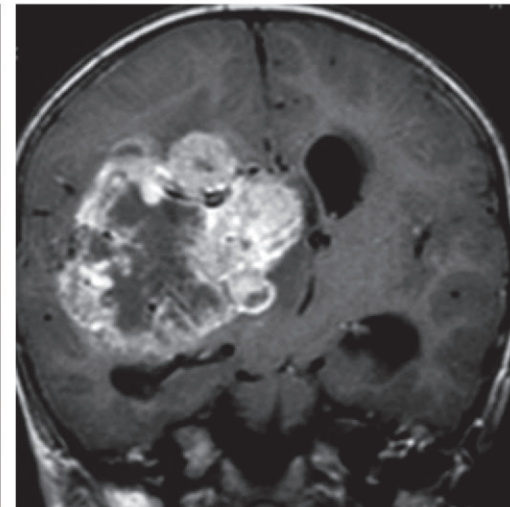
Figure 16. (a) Photomicrograph (original magnification, $\times 200$; H-E stain) of a CPC shows increased cellularity, loss of the papillary pattern, and mitotic figures (arrows). (b) Autopsy photograph from a patient with CPC shows a large mass filling the right lateral ventricle. Central yellowish discoloration corresponds to necrosis, and areas of darker discoloration correspond to hemorrhage. (c) Coronal contrast-enhanced T1-weighted image from the same patient as in b shows lack of enhancement centrally, a finding that corresponds to the area of necrosis.



a.



b.



c.

more than five mitoses per high-power field, increased cellular density, nuclear pleomorphism, blurring of the papillary pattern, and necrosis (40) (Fig 16a). At gross inspection, these tumors may appear fleshy with areas of necrosis and hemorrhage (40) (Fig 16b, 16c).

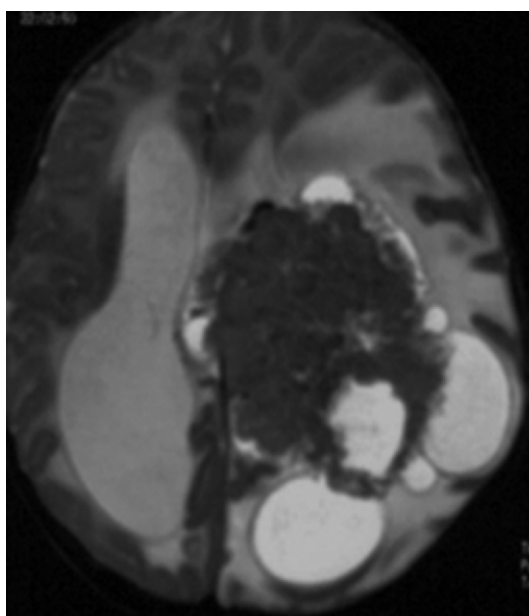
Imaging Features

Teaching Point
Imaging alone does not allow distinction between these neoplasms. All of them may demonstrate CSF dissemination; therefore, imaging of the entire neuroaxis is recommended (52,53) (Fig 17). Choroid plexus neoplasms are very vascular lesions that demonstrate avid enhancement at contrast-enhanced imaging. They are iso- to hyperattenuating at CT. CT angiography as well as conventional angiography may reveal an enlarged choroidal artery if the neoplasm is in the atrium

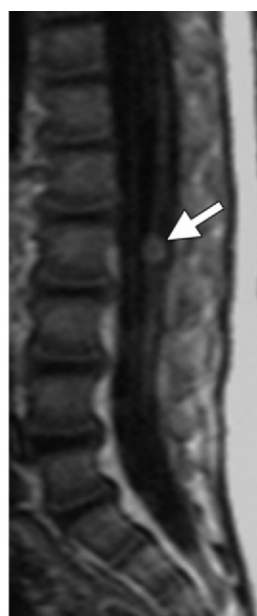
of the lateral ventricle. Calcifications and foci of hemorrhage may be seen, and hydrocephalus commonly occurs.

CPP and atypical CPP frequently have a papillary or lobulated appearance, which helps differentiate them from other intraventricular neoplasms; conversely, carcinomas tend to have a more irregular contour (Fig 18a, 18b) (54). Cystic areas may be present within the tumor. Septa or cysts may also occur within the ventricular system, possibly reflecting an inflammatory reaction to the tumor or related to tumoral hemorrhage (54). At MR imaging, these lesions are iso- to hypointense on T1-weighted images and iso- to hyperintense on T2-weighted images; flow voids are common.

Choroid plexus neoplasms may have a long vascular pedicle, which may twist, leading to tumor infarction. Periventricular vasogenic edema may occur in all choroid plexus tumors, and a suggestion of parenchymal invasion may also be seen at imaging in all three tumor types.

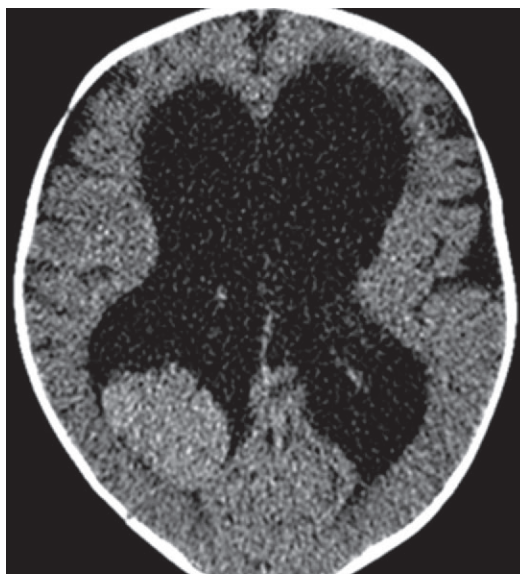


a.

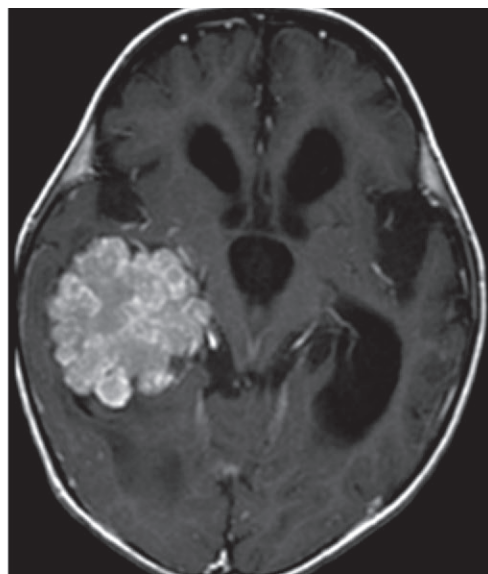


b.

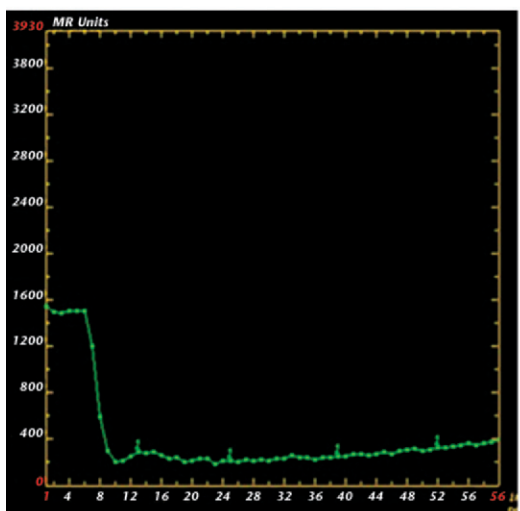
Figure 17. CPC in an 18-month-old boy. **(a)** Axial T2-weighted image shows a large heterogeneous mass with cystic and solid components arising from the lateral ventricle with surrounding vasogenic edema. Hydrocephalus is present. **(b)** Sagittal contrast-enhanced T1-weighted image shows an enhancing nodule (arrow) along the cauda equina, a finding consistent with CSF dissemination.



a.



b.



c.

Figure 18. CPP in a 9-month-old boy. **(a)** Axial nonenhanced CT image shows a lobulated slightly hyperattenuating mass in the atrium of the right lateral ventricle. Hydrocephalus is present. **(b)** Axial contrast-enhanced T1-weighted image shows avid enhancement of the mass. **(c)** Dynamic perfusion imaging graph of signal intensity versus volume, obtained with the dynamic susceptibility contrast technique, shows markedly elevated blood flow (decreased values along the y-axis) with lack of return to the baseline, findings consistent with retention of contrast material within the tumor interstitium.

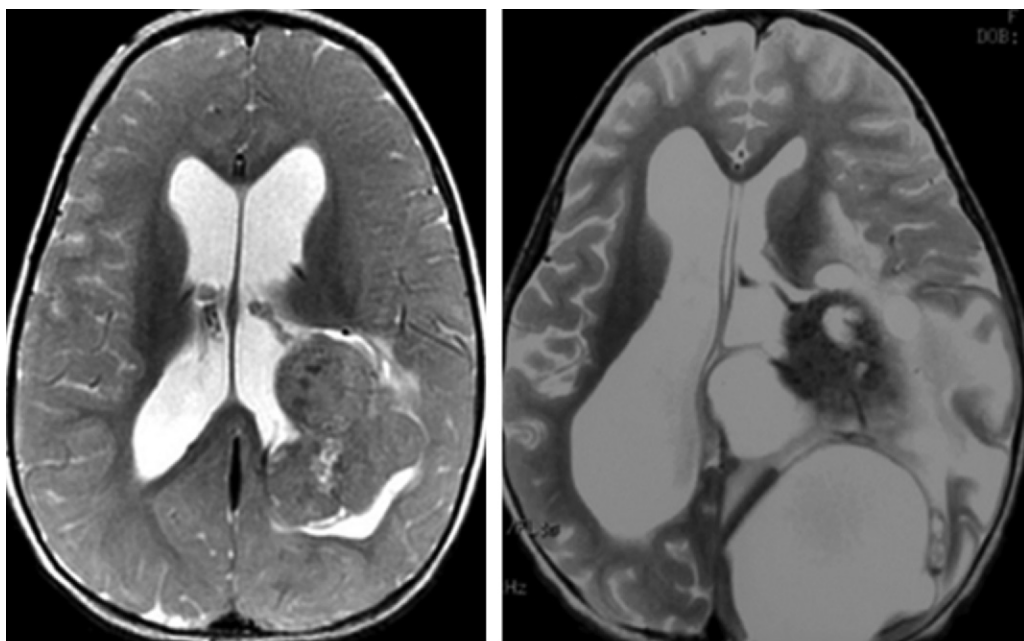
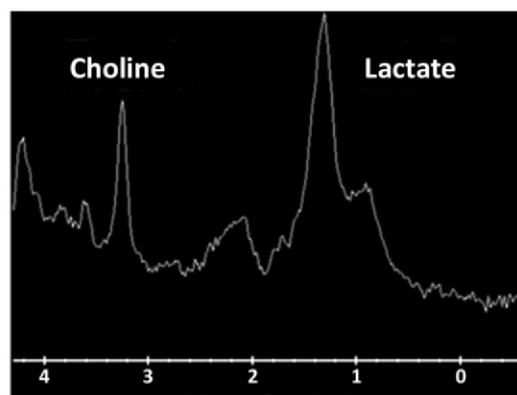
**a.**

Figure 19. Choroid plexus tumors. **(a)** Axial T2-weighted image of a 9-month-old boy with new-onset tonic-clonic seizures shows a lobulated neoplasm in the atrium of the left lateral ventricle. Minimal increased signal intensity is seen in the adjacent brain parenchyma. Histologic analysis demonstrated a CPC. **(b)** Graph from short-echo MR spectroscopy of the patient in **a** shows elevated choline and lactate peaks. **(c)** Axial T2-weighted image of an 8-month-old boy with enlarging head circumference shows a heterogeneous cystic and solid mass with a marked degree of surrounding vasogenic edema. Histologic analysis demonstrated a CPP.

c.**b.**

Perfusion imaging reflects the high blood flow through these neoplasms; owing to lack of a blood-brain barrier, contrast material persists within the interstitium (Fig 18c) (54).

MR spectroscopy of choroid plexus tumors demonstrates a marked choline peak without an N-acetylaspartate or creatine peak; carcinomas also demonstrate elevation of the lactate level (55). CPCs tend to be more heterogeneous than CPPs at CT and MR imaging, in part reflecting areas of necrosis; however, there is considerable overlap in the imaging findings between CPP, atypical CPP, and CPC, and some CPCs may have a very benign imaging appearance (1) (Fig 19).

Meningioma

Intraventricular meningiomas account for 0.5%–3.7% of intracranial meningiomas (56). They are believed to arise from arachnoidal cap cells trapped in the choroid plexus or from the tela choroidea during embryologic formation of the choroid fissure and plexus (1,57). The most common location for intraventricular meningiomas is in the atrium of the lateral ventricles (1). Less commonly, they may arise in the third ventricle and rarely in the fourth ventricle (56).

Like meningiomas elsewhere, they are most common in females (female-to-male ratio, 2:1)

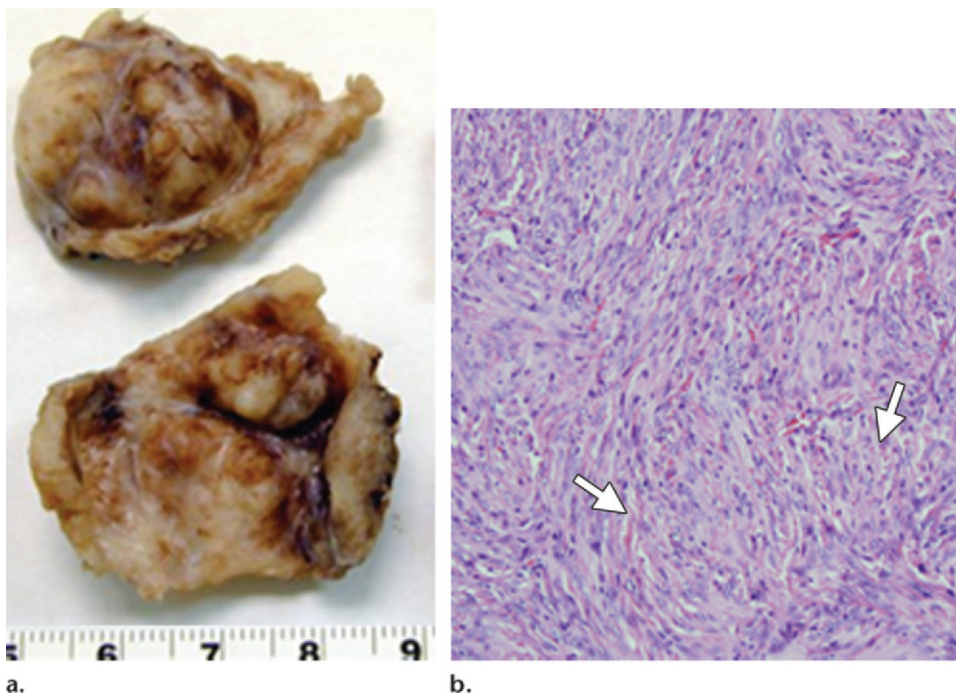


Figure 20. Intraventricular meningioma in a 16-year-old boy with loss of consciousness. **(a)** Photograph of the resected meningioma reveals a well-circumscribed mass. (Scale is in centimeters.) **(b)** Photomicrograph (original magnification, $\times 50$; H-E stain) shows large uniform cells. Minimal whorl formation is present (arrows).

with a peak age range of 30–60 years (58,59). Meningiomas can also rarely affect the pediatric age group, accounting for less than 3% of intracranial neoplasms in this population. However, the intraventricular form accounts for 17% of pediatric meningiomas. **No gender predilection is seen in the pediatric age group, but there is a higher risk of sarcomatous change, and the possibility of associated neurofibromatosis type 2 should be considered (54,60).**

These neoplasms usually reach a large size before patients become symptomatic; patients typically present with signs of increased intracranial pressure but may also present with contralateral sensory or motor deficits (1,56). Rare reports exist of intraventricular hemorrhage secondary to an intraventricular meningioma (61). Most intraventricular meningiomas demonstrate indolent biologic behavior, but rarely cases of atypical or anaplastic lesions have been reported. Also, CSF or hematogenous metastases have rarely been reported regardless of tumor grade (62,63).

Teaching Point

Pathologic Findings

Gross inspection reveals a well-demarcated rubbery or firm mass (Fig 20a). There is no difference in terms of histologic features between an intraventricular meningioma and one arising from a dural attachment. In adults, most intraventricular meningiomas are benign and of the meningotheelial type. This form resembles the arachnoidal cap cell, consisting of uniform cells with oval nuclei containing delicate chromatin that may occasionally demonstrate central clearing. Psammoma bodies are not common. Another common histopathologic subtype is fibroblastic, but other forms have also been described.

Imaging Features

CT reveals a well-defined, iso- to hyperattenuating globular mass (Fig 21a). MR imaging demonstrates a mass that is iso- to hypointense on T1-weighted images and iso- to hyperintense on T2-weighted images (Fig 21b). Owing to the

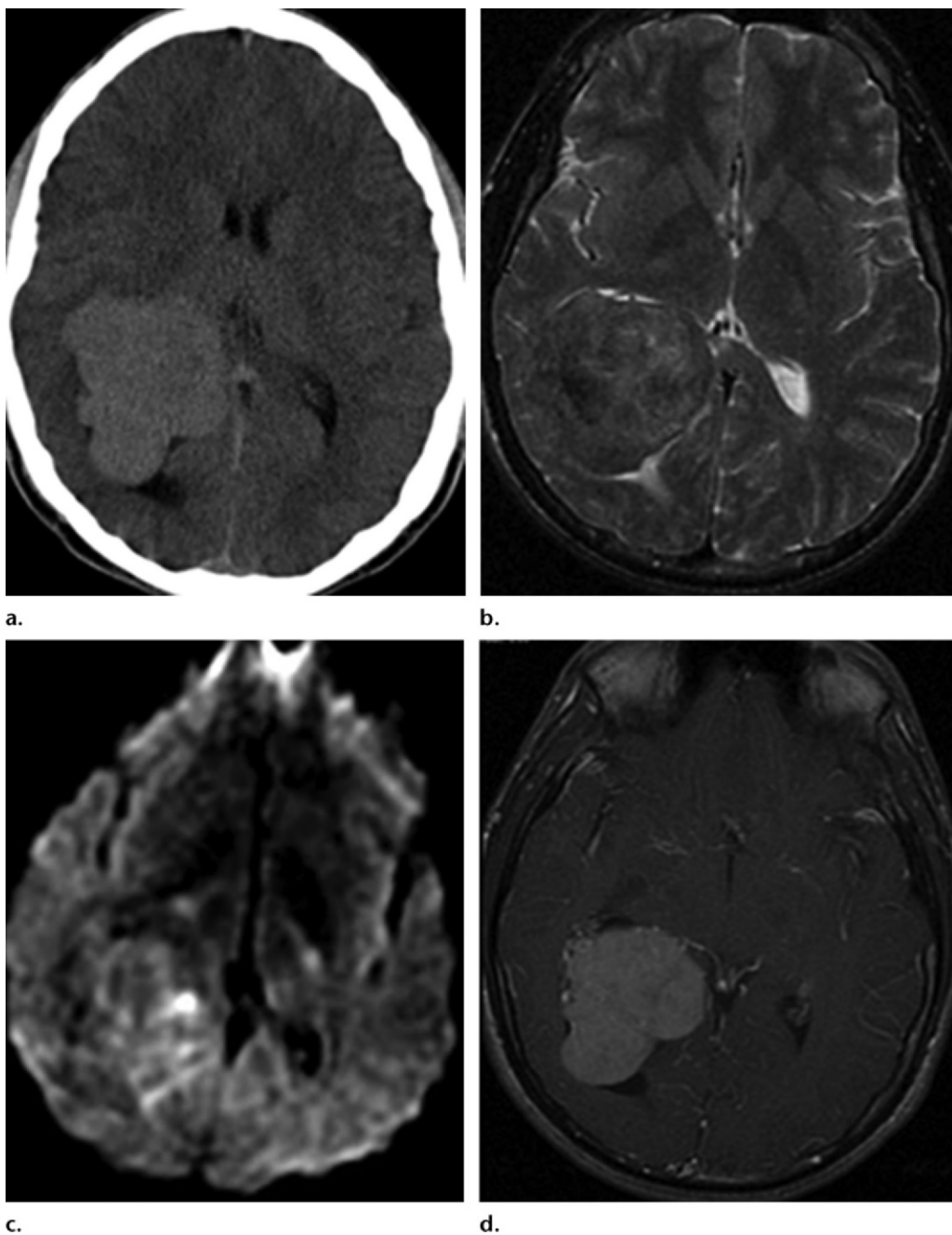


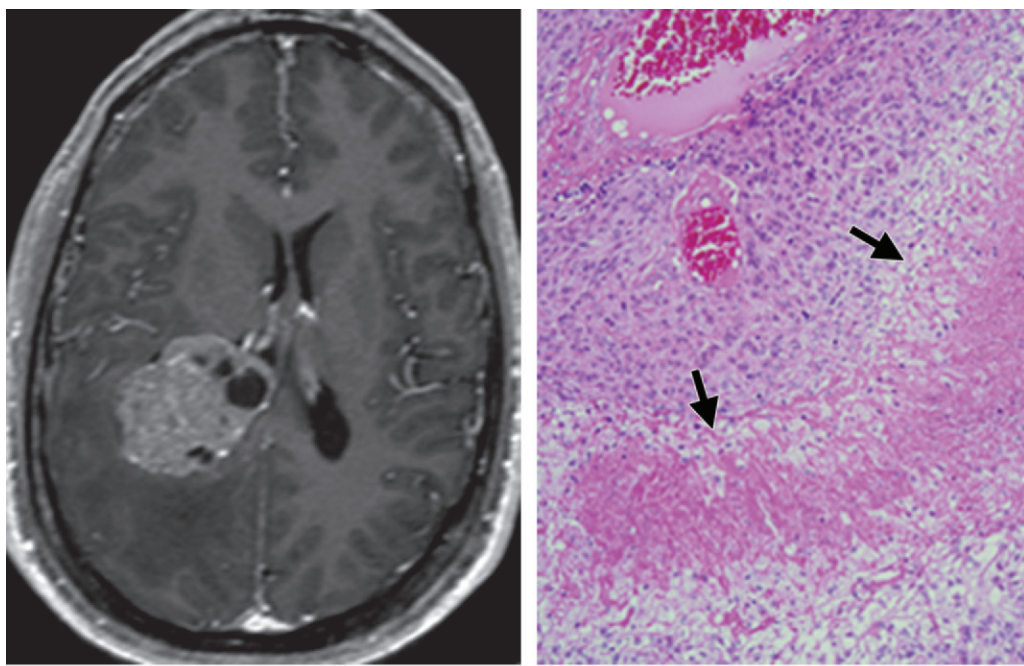
Figure 21. Intraventricular meningioma in a 16-year-old boy with loss of consciousness. **(a)** Axial nonenhanced CT image shows a hyperattenuating mass in the atrium of the right lateral ventricle. **(b)** Axial T2-weighted image shows a slightly heterogeneous, predominantly isointense mass. No surrounding edema is present. **(c)** Axial diffusion-weighted image shows foci of reduced diffusion. **(d)** Axial contrast-enhanced T1-weighted image shows avid homogeneous enhancement.

highly vascular nature of these lesions, avid enhancement is seen on contrast-enhanced images (Fig 21d).

Local or diffuse ventricular dilatation may be present, depending on the degree of obstruction of CSF flow. Periventricular edema may be seen, which has been speculated to be secondary to

reversal of transependymal CSF flow or to secretion of vascular endothelial growth factor by the meningioma, thus inducing the edema (1,64). Reduced diffusion may be seen in some meningiomas, possibly reflecting high cellular density; however, this has not been found useful in predicting grade or histologic subtype (65) (Fig 21c).

Calcification may be present in approximately 50% of cases, and cystic areas may also be pres-



a.

b.

Figure 22. Anaplastic intraventricular meningioma in a 38-year-old man with a 2-week history of headaches. **(a)** Axial contrast-enhanced T1-weighted image shows an enhancing mass with cystic foci in the atrium of the right lateral ventricle. Surrounding vasogenic edema is present. **(b)** Photomicrograph (original magnification, $\times 100$; H-E stain) shows areas of necrosis (arrows), which may be seen in the anaplastic variant and most likely contributed to the cystic appearance.

ent (1). It has been reported that cystic areas are more common in the pediatric population than in adults (66,67). The possible causes of cyst formation include necrosis, cystic degeneration, active secretion by tumor cells, and intratumoral hemorrhage (68) (Fig 22).

MR spectroscopy reveals elevated choline level with variable amounts of lactate, lipid, and alanine (doublet centered at 1.47 ppm). *N*-acetylaspartate and creatine levels are reduced (69). At perfusion-weighted imaging, meningiomas demonstrate high blood volume and persistence of contrast material within the tumor interstitium due to lack of a blood-brain barrier (54).

Chordoid Glioma

Chordoid glioma is a WHO grade II, slow-growing glial neoplasm described in 1998 by Brat et al (70) that involves the region of the anterior third ventricle and the hypothalamus. These are rare lesions and therefore demographic information is limited, but a female predominance (female-to-male ratio, 2:1 to 3:1) and a mean age of 46 years are reported (71,72). Two cases of chordoid glioma in children have been reported (73,74).

Given the location, patients typically present with hypothalamic dysfunction, homonymous hemianopsia, or increased intracranial pressure. Although this is described as a noninfiltrating le-

sion, a recent case report described infiltration of the optic chiasm (75). Gross total resection has been reported to result in disease-free survival, but this frequently cannot be achieved due to the location (76). Unfortunately, without gross total resection the recurrence rate is high (77).

Pathologic Findings

The cell of origin is unknown, although there is speculation that chordoid gliomas may arise from the tanycytes, which are special ependymal cells located in the floor of the third ventricle (78,79). This neoplasm received its name because of a histologic appearance similar to that of chordomas. Vacuolization within the mucin-rich stroma resembles the mucin-rich matrix seen in chordomas (Fig 23a).

At gross inspection, chordoid gliomas are well-circumscribed firm tumors with a pushing border. The neoplasm is composed of clusters and chords of oval to polygonal epithelioid tumor cells. Mitotic figures, necrosis, and vascular proliferation are rare (80,81). Chordoid gliomas stain avidly with the glial cell marker glial fibrillary acidic protein (GFAP), which is a protein expressed by numerous cell types of the central nervous system.

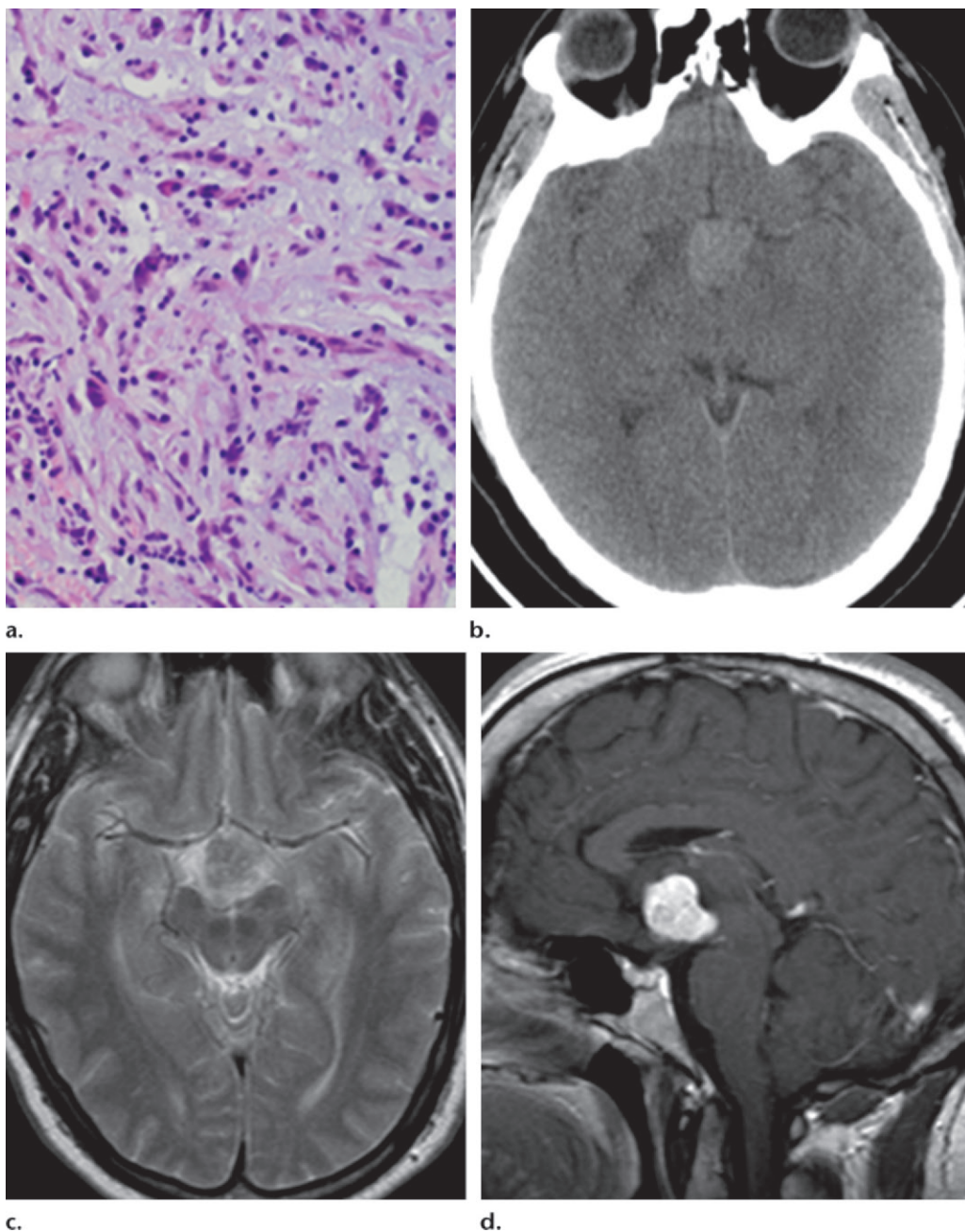
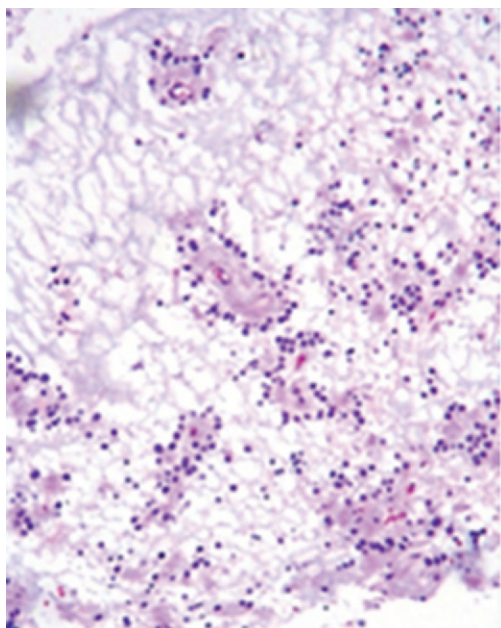


Figure 23. Chordoid glioma in a 32-year-old woman with blurry vision. **(a)** Photomicrograph (original magnification, $\times 200$; H-E stain) shows chordoid architecture and round to oval nuclei in a myxoid background. **(b)** Axial nonenhanced CT image shows a hyperattenuating lesion that appears to project into the suprasellar region. Mild edema is noted in the adjacent brain parenchyma. **(c)** On an axial T2-weighted image, the lesion is isointense to gray matter. **(d)** Sagittal contrast-enhanced T1-weighted image shows an avidly enhancing, well-circumscribed mass along the anterior aspect of the third ventricle.

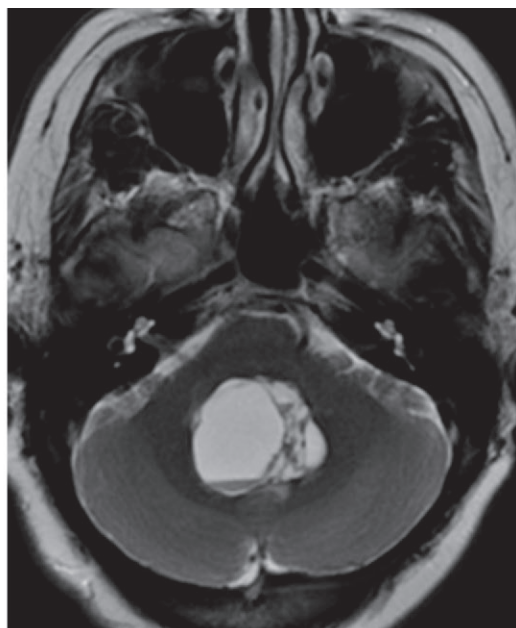
Imaging Features

Chordoid glioma is a well-circumscribed ovoid lesion in the region of the anterior third ventricle and hypothalamus. These neoplasms are hyper-

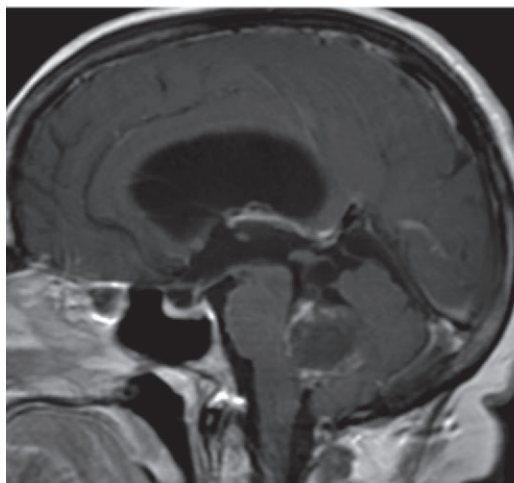
attenuating at CT (Fig 23b). At MR imaging, chordoid gliomas are isointense to gray matter on T1-weighted images and hyperintense on T2-weighted images (Fig 23c) and enhance avidly after contrast material administration (Fig 23d). Perilesional edema may be present. Cystic changes within the lesion occasionally occur, but intratumoral calcifications are rare (82).



a.



b.



c.

Rosette-forming Glioneuronal Tumor

RGNT is a recently described WHO grade I, rare primary brain tumor. It was included as a distinct glioneuronal neoplasm in the 2007 WHO classification of tumors of the central nervous system. These neoplasms demonstrate glial and neuronal differentiation, and it has been suggested that they arise from progenitor pluripotential cells of the subependymal plate (83).

RGNTs typically occur in young adults (mean age, 31.5 years), demonstrate indolent behavior, and do not tend to recur after surgical resection. Patients usually present with signs of increased intracranial pressure or ataxia, and gross total resection is usually curative (84). Distant CSF spread has not been reported, to our knowledge, but one case of intraventricular spread has been

Figure 24. RGNT in a 57-year-old woman with multiple episodes of presyncope. **(a)** Photomicrograph (original magnification, $\times 100$; H-E stain) shows small uniform neurocytes forming small rosettes within a loose mucoid matrix. The glial component (not seen) resembles pilocytic astrocytoma. **(b)** Axial T2-weighted image shows a predominantly cystic mass involving the fourth ventricle. Layered blood is noted in the dependent portion. **(c)** Sagittal contrast-enhanced T1-weighted image shows minimal enhancement involving the periphery of the lesion. Hydrocephalus is present.

described (85). There is a female predominance (female-to-male ratio, 1.75:1) (84).

RGNTs were originally described as solely occurring in the fourth ventricle, but a recent case report describes an RGNT attached to the septum pellucidum (86). Rare extraventricular locations have been reported as well, including the suprasellar region and spinal cord (87).

Pathologic Findings

At histologic examination, the tumor is biphasic. The low-grade glial component resembles pilocytic astrocytoma, with astrogliosis, bipolar astrocytes, and eosinophilic granular bodies and Rosenthal fibers. The neurocytic component is composed of small uniform neurocytes with round nuclei and a fine stippled chromatin pattern that form small neurocytic rosettes. Mitotic activity and necrosis are absent (Fig 24a) (88).

Imaging Features

Imaging reveals a fairly well-circumscribed, heterogeneous solid and cystic mass classically centered on the fourth ventricle (Fig 24b). Heterogeneous enhancement is seen on contrast-enhanced images (Fig 24c). Intratumoral hemorrhage and calcification may occur (87,89). Although this is an uncommon neoplasm, the diagnosis of RGNT should be considered when a cystic neoplasm of the fourth ventricle is encountered in an adult.

Metastases and Other Intraventricular Neoplasms

Intraventricular metastases account for 0.9%–4.6% of cerebral metastases (1). In adults, renal, colon, and lung carcinoma are the most common causes; in children, neuroblastoma, Wilms tumor, and retinoblastoma are most common (1,90). Renal cell carcinoma is remarkable in its ability to produce solitary metastases up to 50 years after identification of the primary lesion (91).

Intraventricular metastases are most common in the lateral ventricles but may also occur in the third ventricle and very rarely in the fourth ventricle (1). Imaging findings of a solitary metastasis to the choroid plexus may be indistinguishable from those of a meningioma or choroid plexus neoplasm, and a history of a primary neoplasm should raise suspicion for metastasis. Avid enhancement is usually seen on contrast-enhanced images, and vasogenic edema may be seen in the adjacent brain parenchyma.

Many other neoplasms involve the ventricular system, including lymphoma, low- and high-grade gliomas, intraventricular craniopharyngioma, and primitive neuroectodermal tumor (92).

Conclusions

A wide variety of neoplasms involve the ventricular system. Many have similar imaging appearances, making the imaging findings less helpful in narrowing the differential diagnosis; however, recent articles suggest that MR spectroscopy may aid in differentiation of the diagnosis (23). Consideration of the tumor location and the patient's

age and gender in combination with the imaging findings is currently the best method for narrowing the differential diagnosis.

References

- Koeller KK, Sandberg GD. Cerebral intraventricular neoplasms: radiologic-pathologic correlation. *RadioGraphics* 2002;22(6):1473–1505.
- Spoto GP, Press GA, Hesselink JR, Solomon M. Intracranial ependymoma and subependymoma: MR manifestations. *AJR Am J Roentgenol* 1990;154(4):837–845.
- Teo C, Nakaji P, Symons P, Tobias V, Cohn R, Smee R. Ependymoma. *Childs Nerv Syst* 2003;19(5–6):270–285.
- Yuh EL, Barkovich AJ, Gupta N. Imaging of ependymomas: MRI and CT. *Childs Nerv Syst* 2009;25(10):1203–1213.
- Wiestler O, Schiffer D, Coons S, Prayson R, Rosenblum M. Ependymoma. In: Kleihues P, Cavenee WK, eds. *Pathology and genetics of tumours of the nervous system*. Lyon, France: IARC, 2000; 72–76.
- Ma L, Xiao SY, Liu XS, You C, Zhang YK. Intracranial extraaxial ependymoma in children: a rare case report and review of the literature. *Neurol Sci* 2012;33(1):151–154.
- Phi JH, Wang KC, Park SH, et al. Pediatric infratentorial ependymoma: prognostic significance of anaplastic histology. *J Neurooncol* 2012;106(3):619–626.
- Pejavar S, Polley MY, Rosenberg-Wohl S, et al. Pediatric intracranial ependymoma: the roles of surgery, radiation and chemotherapy. *J Neurooncol* 2012;106(2):367–375.
- Armington WG, Osborn AG, Cubberley DA, et al. Supratentorial ependymoma: CT appearance. *Radiology* 1985;157(2):367–372.
- Salazar OM. A better understanding of CNS seeding and a brighter outlook for postoperatively irradiated patients with ependymomas. *Int J Radiat Oncol Biol Phys* 1983;9(8):1231–1234.
- Wiestler O, Shiffer D. Subependymoma. In: Kleihues P, Cavenee WK, eds. *Pathology and genetics of tumours of the nervous system*. Lyon, France: IARC, 2000; 80–81.
- Rushing EJ, Cooper PB, Quezado M, et al. Subependymoma revisited: clinicopathological evaluation of 83 cases. *J Neurooncol* 2007;85(3):297–305.
- Fujisawa H, Hasegawa M, Ueno M. Clinical features and management of five patients with supratentorial subependymoma. *J Clin Neurosci* 2010;17(2):201–204.
- Lombardi D, Scheithauer BW, Meyer FB, et al. Symptomatic subependymoma: a clinicopathological and flow cytometric study. *J Neurosurg* 1991;75(4):583–588.

15. Ragel BT, Osborn AG, Whang K, Townsend JJ, Jensen RL, Couldwell WT. Subependymomas: an analysis of clinical and imaging features. *Neurosurgery* 2006;58(5):881–890; discussion 881–890.
16. Hassoun J, Gambarelli D, Grisoli F, et al. Central neurocytoma: an electron-microscopic study of two cases. *Acta Neuropathol (Berl)* 1982;56(2):151–156.
17. Figarella-Branger D, Soylemezoglu F, Kleihues P, Hassoun J. Central neurocytoma. In: Kleihues P, Cavenee WK, eds. *Pathology and genetics of tumours of the nervous system*. Lyon, France: IARC, 2000; 107–109.
18. Chen H, Zhou R, Liu J, Tang J. Central neurocytoma. *J Clin Neurosci* 2012;19(6):849–853.
19. Tomura N, Hirano H, Watanabe O, et al. Central neurocytoma with clinically malignant behavior. *AJNR Am J Neuroradiol* 1997;18(6):1175–1178.
20. Ando K, Ishikura R, Morikawa T, et al. Central neurocytoma with craniospinal dissemination. *Magn Reson Med Sci* 2002;1(3):179–182.
21. Louis DN, Ohgaki H, Wiestler OD, et al. The 2007 WHO classification of tumours of the central nervous system. *Acta Neuropathol (Berl)* 2007;114(2):97–109.
22. Robbins P, Segal A, Narula S, et al. Central neurocytoma: a clinicopathological, immunohistochemical and ultrastructural study of 7 cases. *Pathol Res Pract* 1995;191(2):100–111.
23. Shah T, Jayasundar R, Singh VP, Sarkar C. In vivo MRS study of intraventricular tumors. *J Mag Reson Imaging* 2011;34(5):1053–1059.
24. Shah T, Jayasundar R, Singh VP, Sarkar C. MRS characterization of central neurocytomas using glycine. *NMR Biomed* 2011;24(10):1408–1413.
25. Liu M, Yue Q, Isobe T, et al. Proton MR spectroscopy of central neurocytoma using short and long echo time: new proofs for the existence of glycine and glutamate. *Acad Radiol* 2012;19(7):779–784.
26. Wiestler O, Lopes B, Green A, Vinters H. Tuberous sclerosis complex and subependymal giant cell astrocytoma. In: Kleihues P, Cavenee WK, eds. *Pathology and genetics of tumours of the nervous system*. Lyon, France: IARC, 2000; 227–230.
27. Berhouma M. Management of subependymal giant cell tumors in tuberous sclerosis complex: the neurosurgeon's perspective. *World J Pediatr* 2010;6(2):103–110.
28. Kim SK, Wang KC, Cho BK, et al. Biological behavior and tumorigenesis of subependymal giant cell astrocytomas. *J Neurooncol* 2001;52(3):217–225.
29. Curatolo P, Bombardieri R, Jozwiak S. Tuberous sclerosis. *Lancet* 2008;372(9639):657–668.
30. Takei H, Adesina AM, Powell SZ. Solitary subependymal giant cell astrocytoma incidentally found at autopsy in an elderly woman without tuberous sclerosis complex. *Neuropathology* 2009;29(2):181–186.
31. Kwiatkowska J, Wigowska-Sowinska J, Napierala D, Slomski R, Kwiatkowski DJ. Mosaicism in tuberous sclerosis as a potential cause of the failure of molecular diagnosis. *N Engl J Med* 1999;340(9):703–707.
32. Shepherd CW, Scheithauer BW, Gomez MR, Altermatt HJ, Katzmann JA. Subependymal giant cell astrocytoma: a clinical, pathological, and flow cytometric study. *Neurosurgery* 1991;28(6):864–868.
33. Bollo RJ, Berliner JL, Fischer I, et al. Extraventricular subependymal giant cell tumor in a child with tuberous sclerosis complex. *J Neurosurg Pediatr* 2009;4(1):85–90.
34. Sharma MC, Ralte AM, Gaekwad S, Santosh V, Shankar SK, Sarkar C. Subependymal giant cell astrocytoma: a clinicopathological study of 23 cases with special emphasis on histogenesis. *Pathol Oncol Res* 2004;10(4):219–224.
35. Teljeian AE, Judkins A, Younkin D, Pollock AN, Crino P. Subependymal giant cell astrocytoma with cranial and spinal metastases in a patient with tuberous sclerosis: case report. *J Neurosurg* 2004;100(5 suppl pediatrics):498–500.
36. Grajkowska W, Kotulska K, Jurkiewicz E, et al. Subependymal giant cell astrocytomas with atypical histological features mimicking malignant gliomas. *Folia Neuropathol* 2011;49(1):39–46.
37. Clarke MJ, Foy AB, Wetjen N, Raffel C. Imaging characteristics and growth of subependymal giant cell astrocytomas. *Neurosurg Focus* 2006;20(1):E5.
38. Buccoliero AM, Franchi A, Castiglione F, et al. Subependymal giant cell astrocytoma (SEGA): is it an astrocytoma? Morphological, immunohistochemical and ultrastructural study. *Neuropathology* 2009;29(1):25–30.
39. Wolff JE, Finlay JL. Choroid plexus tumors. In: Carroll WL, Finlay JL, eds. *Cancer in children and adolescents*. Sudbury, Mass: Jones & Bartlett, 2009; 299.
40. Paulus W, Brandner S. Choroid plexus tumors. In: Louis DN, Ohgaki H, Wiestler OD, Cavenee WK, eds. *WHO classification of tumours of the central nervous system*. Lyon, France: IARC, 2007; 82–85.
41. Aguzzi A, Brandner S, Paulus W. Choroid plexus tumours. In: Kleihues P, Cavenee WK, eds. *Pathology and genetics of tumours of the nervous system*. Lyon, France: IARC, 2000; 84–86.
42. Stafrace S, Molloy J. Extraventricular choroid plexus papilloma in a neonate. *Pediatr Radiol* 2008;38(5):593.
43. Stevens EA, Stanton CA, Nichols K, Ellis TL. Rare intraparenchymal choroid plexus carcinoma resembling atypical teratoid/rhabdoid tumor diagnosed by immunostaining for INI1 protein. *J Neurosurg Pediatr* 2009;4(4):368–371.

44. Frye RE, Polling JS, Ma LCK. Choroid plexus papilloma expansion over 7 years in Aicardi syndrome. *J Child Neurol* 2007;22(4):484–487.
45. Gozali AE, Britt B, Shane L, et al. Choroid plexus tumors: management, outcome, and association with the Li-Fraumeni syndrome—the Children's Hospital Los Angeles (CHLA) experience, 1991–2010. *Pediatr Blood Cancer* 2012;58(6):905–909.
46. Chow E, Jenkins JJ, Burger PC, et al. Malignant evolution of choroid plexus papilloma. *Pediatr Neurosurg* 1999;31(3):127–130.
47. Kishore S, Negi G, Meena H, Anuradha K, Pathak PV, Bansal K. Choroid plexus carcinoma in an adult. *J Neurosci Rural Pract* 2012;3(1):71–73.
48. Osada H, Mori K, Yamamoto T, Nakao Y, Wada R, Maeda M. Choroid plexus carcinoma secreting carbohydrate antigen 19-9 in an adult: case report. *Neurol Med Chir (Tokyo)* 2006;46(5):251–253.
49. Lozier AP, Arbaje YM, Scheithauer BW. Supratentorial, extraventricular choroid plexus carcinoma in an adult: case report. *Neurosurgery* 2009;65(4):E816–E817.
50. Rickert CH, Wiestler OD, Paulus W. Chromosomal imbalances in choroid plexus tumors. *Am J Pathol* 2002;160(3):1105–1113.
51. Meyers SP, Khademian ZP, Chuang SH, Pollack IF, Korones DN, Zimmerman RA. Choroid plexus carcinomas in children: MRI features and patient outcomes. *Neuroradiology* 2004;46(9):770–780.
52. Irsutti M, Thorn-Kany M, Arrué P, et al. Suprasellar seeding of a benign choroid plexus papilloma of the fourth ventricle with local recurrence. *Neuroradiology* 2000;42(9):657–661.
53. Uff CEG, Galloway M, Bradford R. Metastatic atypical choroid plexus papilloma: a case report. *J Neurooncol* 2007;82(1):69–74.
54. Barkovich AJ. Pediatric neuroimaging. 4th ed. Philadelphia, Pa: Lippincott Williams & Williams, 2005; 603–610.
55. Horská A, Ulug AM, Melhem ER, et al. Proton magnetic resonance spectroscopy of choroid plexus tumors in children. *J Magn Reson Imaging* 2001;14(1):78–82.
56. Liu M, Wei Y, Liu Y, Zhu S, Li X. Intraventricular meningiomas: a report of 25 cases. *Neurosurg Rev* 2006;29(1):36–40.
57. Guidetti B, Delfini R, Gagliardi FM, Vagozzini R. Meningiomas of the lateral ventricles: clinical, neuroradiologic, and surgical considerations in 19 cases. *Surg Neurol* 1985;24(4):364–370.
58. Crisculo GR, Symon L. Intraventricular meningioma: a review of 10 cases of the National Hospital, Queen Square (1974–1985) with reference to the literature. *Acta Neurochir (Wien)* 1986;83(3–4): 83–91.
59. Fornari M, Savoardo M, Morello G, Solero CL. Meningiomas of the lateral ventricles: neuroradiological and surgical considerations in 18 cases. *J Neurosurg* 1981;54(1):64–74.
60. Im SH, Wang KC, Kim SK, et al. Childhood meningioma: unusual location, atypical radiological findings, and favorable treatment outcome. *Childs Nerv Syst* 2001;17(11):656–662.
61. Fu Z, Xu K, Xu B, Qu L, Yu J. Lateral ventricular meningioma presenting with intraventricular hemorrhage: a case report and literature review. *Int J Med Sci* 2011;8(8):711–716.
62. Shintaku M, Hashimoto K, Okamoto S. Intraventricular meningioma with anaplastic transformation and metastasis via the cerebrospinal fluid. *Neuropathology* 2007;27(5):448–452.
63. Fulkerson DH, Horner TG, Hatab EM. Histologically benign intraventricular meningioma with concurrent pulmonary metastasis: case report and review of the literature. *Clin Neurol Neurosurg* 2008; 110(4):416–419.
64. Ding YS, Wang HD, Tang K, Hu ZG, Jin W, Yan W. Expression of vascular endothelial growth factor in human meningiomas and peritumoral brain areas. *Ann Clin Lab Sci* 2008;38(4):344–351.
65. Santelli L, Ramondo G, Della Puppa A, et al. Diffusion-weighted imaging does not predict histological grading in meningiomas. *Acta Neurochir (Wien)* 2010;152(8):1315–1319; discussion 1319.
66. Reddy DR, Kolluri VRS, Rao KS, et al. Cystic meningiomas in children. *Childs Nerv Syst* 1986;2(6): 317–319.
67. Starshak RJ. Cystic meningiomas in children: a diagnostic challenge. *Pediatr Radiol* 1996;26(10): 711–714.
68. Zee CS, Chen T, Hinton DR, Tan M, Segall HD, Apuzzo ML. Magnetic resonance imaging of cystic meningiomas and its surgical implications. *Neurosurgery* 1995;36(3):482–488.

69. Majós C, Cucurella G, Aguilera C, Coll S, Pons LC. Intraventricular meningiomas: MR imaging and MR spectroscopic findings in two cases. *AJNR Am J Neuroradiol* 1999;20(5):882–885.
70. Brat DJ, Scheithauer BW, Staugaitis SM, Cortez SC, Brecher K, Burger PC. Third ventricular chordoid glioma: a distinct clinicopathologic entity. *J Neuropathol Exp Neurol* 1998;57(3):283–290.
71. Desouza RM, Bodi I, Thomas N, Marsh H, Crocker M. Chordoid glioma: ten years of a low-grade tumor with high morbidity. *Skull Base* 2010;20(2):125–138.
72. Buccoliero AM, Caldarella A, Gallina P, Di Lorenzo N, Taddei A, Taddei GL. Chordoid glioma: clinicopathologic profile and differential diagnosis of an uncommon tumor. *Arch Pathol Lab Med* 2004;128(11):e141–e145.
73. Castellano-Sánchez AA, Schemankewitz E, Mazewski C, Brat DJ. Pediatric chordoid glioma with chondroid metaplasia. *Pediatr Dev Pathol* 2001;4(6):564–567.
74. Jain D, Sharma MC, Sarkar C, et al. Chordoid glioma: report of two rare examples with unusual features. *Acta Neurochir (Wien)* 2008;150(3):295–300; discussion 300.
75. Al Hinai QS, Petrecca K. Rarest of the rare: chordoid glioma infiltrating the optic chiasm. *Surg Neurol Int* 2011;2:53.
76. Raizer JJ, Shetty T, Gutin PH, et al. Chordoid glioma: report of a case with unusual histologic features, ultrastructural study and review of the literature. *J Neurooncol* 2003;63(1):39–47.
77. Jung TY, Jung S. Third ventricular chordoid glioma with unusual aggressive behavior. *Neurol Med Chir (Tokyo)* 2006;46(12):605–608.
78. Brat DJ. The elusive origin of chordoid glioma. *Arch Pathol Lab Med* 2006;130(4):437–438.
79. Leeds NE, Lang FF, Ribalta T, Sawaya R, Fuller GN. Origin of chordoid glioma of the third ventricle. *Arch Pathol Lab Med* 2006;130(4):460–464.
80. Brat DJ, Scheithauer BW, Cortez SC, Reifenberger G, Burger PC. Chordoid glioma of the third ventricle. In: Kleihuis P, Cavenee WK, eds. *Pathology and genetics of tumours of the nervous system*. Lyon, France: IARC, 2000; 90–91.
81. Pasquier B, Péoc'h M, Morrison AL, et al. Chordoid glioma of the third ventricle: a report of two new cases, with further evidence supporting an ependymal differentiation, and review of the literature. *Am J Surg Pathol* 2002;26(10):1330–1342.
82. Rees JH. Chordoid glioma of the third ventricle. In: Osborn AG, Salzman KL, Barkovich AJ, eds. *Diagnostic imaging: brain*. 2nd ed. Philadelphia, Pa: Lippincott Williams & Wilkins, 2010; 56–57.
83. Matyja E, Grajkowska W, Nauman P, Ozieblo A, Bonicki W. Rosette-forming glioneuronal tumor of the fourth ventricle with advanced microvascular proliferation: a case report. *Neuropathology* 2011;31(4):427–432.
84. Komori T, Scheithauer BW, Hirose T. A rosette-forming glioneuronal tumor of the fourth ventricle: infratentorial form of dysembryoplastic neuroepithelial tumor? *Am J Surg Pathol* 2002;26(5):582–591.
85. Wang Y, Xiong J, Chu SG, et al. Rosette-forming glioneuronal tumor: report of an unusual case with intraventricular dissemination. *Acta Neuropathol (Berl)* 2009;118(6):813–819.
86. Xiong J, Liu Y, Chu SG, et al. Rosette-forming glioneuronal tumor of the septum pellucidum with extension to the supratentorial ventricles: rare case with genetic analysis. *Neuropathology* 2012;32(3):301–305.
87. Sharma P, Swain M, Padua MD, Ranjan A, Lath R. Rosette-forming glioneuronal tumors: a report of two cases. *Neurol India* 2011;59(2):276–280.
88. Hainfellner JA, Scheithauer BW, Giangaspero F, Rosenblum MK. In: Louis DN, Ohgaki H, Wiestler OD, Cavenee WK, eds. *WHO classification of tumors of the central nervous system*. Lyon, France: IARC, 2007; 115–116.
89. Rosenblum MK. The 2007 WHO classification of nervous system tumors: newly recognized members of the mixed glioneuronal group. *Brain Pathol* 2007;17(3):308–313.
90. Wasita B, Sakamoto M, Mizushima M, Kuroasaki M, Watanabe T. Choroid plexus metastasis from papillary thyroid carcinoma presenting with intraventricular hemorrhage: case report. *Neurosurgery* 2010;66(6):E1213–E1214.
91. Killebrew K, Krigman M, Mahaley MS Jr, Scatliff JH. Metastatic renal cell carcinoma mimicking a meningioma. *Neurosurgery* 1983;13(4):430–434.
92. Oppido PA, Fiorindi A, Benvenuti L, et al. Neuroendoscopic biopsy of ventricular tumors: a multicentric experience. *Neurosurg Focus* 2011;30(4):E2.

From the Radiologic Pathology Archives Intraventricular Neoplasms: Radiologic-Pathologic Correlation

Alice Boyd Smith, MD, Lt Col, USAF MC • James G. Smirniotopoulos, MD • Iren Horkanyne-Szakaly, MD

RadioGraphics 2013; 33:21–43 • Published online 10.1148/rg.331125192 • Content Codes: **CT** **MR** **NR** **OI**

Page 21

Many of these lesions have similar patterns of signal intensity and contrast enhancement at imaging. However, the location of the lesion in the ventricular system—along with knowledge of the patient's age, gender, and underlying conditions—will help narrow the differential diagnosis.

Page 28

Recent evaluation with MR spectroscopy has revealed the presence of glycine (3.55 ppm) within central neurocytomas, a finding that may help differentiate them from other intraventricular neoplasms.

Page 28

SGCT is considered pathognomonic for TS, but there have been rare reports of SGCT in patients without manifestations of TS. However, these cases likely represent somatic mosaicism of the *TS* gene.

Page 32

Imaging alone does not allow distinction between these neoplasms. All of them may demonstrate CSF dissemination; therefore, imaging of the entire neuroaxis is recommended.

Page 35

No gender predilection is seen in the pediatric age group, but there is a higher risk of sarcomatous change, and the possibility of associated neurofibromatosis type 2 should be considered.